Zoological Journal of the Linnean Society, 2022, **XX**, 1–23. With 12 figures.

Anatomy and phylogenetic relationships of *Temnodontosaurus zetlandicus* (Reptilia: Ichthyosauria)

ANTOINE LABOURY[1,*], REBECCA F. BENNION[1,2], BEN THUY[3], ROBERT WEIS[3] and VALENTIN FISCHER[1]

[1]*Evolution & Diversity Dynamics Lab, University of Liège, 14 Allée du 6 Août, Liège 4000, Belgium*
[2]*Palaeontology Department, Royal Belgian Institute of Natural Sciences, 29, Rue Vautier, 1000 Brussels, Belgium*
[3]*Palaeontology Departement, Natural History Museum Luxembourg, 25 Rue Münster, L-2160 Luxembourg, Grand-Duchy of Luxembourg*

Received 25 October 2021; revised 30 November 2021; accepted for publication 4 December 2021

Parvipelvia is a major clade of ichthyosaurians that diversified during the Triassic-Jurassic transition. The interrelationships of early parvipelvians remain unclear and many genera are loosely diagnosed, such as *Temnodontosaurus*, an ecologically important genus from the Early Jurassic of Western Europe. One taxon concentrates many taxonomic issues: '*Ichthyosaurus*' *acutirostris* was previously assigned to *Temnodontosaurus* and for which '*Ichthyosaurus*' *zetlandicus* represents a junior synonym. We redescribe the holotype of '*Ichthyosaurus*' *zetlandicus* (CAMSM J35176) and a new specimen probably attributable to this taxon (MNHNL TU885) from the Toarcian of Luxembourg. We find that ***Temnodontosaurus zetlandicus*** **comb. nov.** is a valid species that should be referred to the genus *Temnodontosaurus*, sharing a number of traits with *Temnodontosaurus nuertingensis* and *Temnodontosaurus trigonodon*, despite having a distinct cranial architecture. Our phylogenetic analyses under both implied weighting maximum parsimony and Bayesian inference recover *T. zetlandicus* as closely related to several species currently assigned to *Temnodontosaurus*. Species included in *Temnodontosaurus* form a polyphyletic yet well-clustered group among basal neoichthyosaurians, demonstrating that the monophyly of this genus needs to be thoroughly investigated.

ADDITIONAL KEYWORDS: *Ichthyosaurus acutirostris* – Lower Jurassic – Luxembourg – Parvipelvia – phylogeny – taxonomy – Toarcian – Whitby – United-Kingdom.

INTRODUCTION

Ichthyosauria is a species-rich clade of marine reptiles that populated ancient oceans from the Early Triassic (Olenekian; e.g. Motani *et al.*, 2017) to the beginning of the Late Cretaceous (Cenomanian-Turonian boundary; Bardet, 1992; Fischer *et al.*, 2016). A single clade of ichthyosaurians, Parvipelvia, is thought to have survived the end-Triassic extinctions (McGowan, 1997; Motani, 2005; Thorne *et al.*, 2011; Fischer *et al.*, 2014; but see Martin *et al.*, 2015) and evolved into a disparate assemblage of forms, filling many roles in the marine ecosystems of the Early Jurassic (Böttcher, 1989; Godefroit, 1994; McGowan, 1996a; Massare, 1997; Martin *et al.*, 2012; Dick & Maxwell, 2015). However, the internal phylogenetic relationships of early parvipelvians appear poorly constrained (Moon, 2017).

Among early parvipelvians, *Temnodontosaurus* Lydekker, 1889 appears to be one of the most problematic genera, being polyphyletic (Moon, 2017) and in dire need of revision, as advocated by multiple authors in the past (McGowan, 1996a; Sander, 2000; Maisch, 2010; Swaby & Lomax, 2020). The current definition of *Temnodontosaurus* stems from phenetic analyses of skull and postcranial shapes in the 1970s (McGowan, 1974). Because skull shape in marine tetrapods is now known to be heavily influenced by ecomorphological convergence (e.g. Kelley & Pyenson, 2015; Fischer, 2016; Fischer *et al.*, 2017, 2020; McCurry *et al.*, 2017), these ratios are likely suboptimal to establish a stable taxonomy. Switching the taxonomy of Early Jurassic ichthyosaurians to apomorphy-based definitions is desirable and ongoing (Maisch & Matzke, 2000; Maisch, 2008, 2010; Martin *et al.*, 2012; Lomax, 2016; Maxwell & Cortés, 2020; Swaby & Lomax, 2020), but still far from complete. Several Early Jurassic ichthyosaurs have been included in *Temnodontosaurus* over the years (McGowan, 1974, 1996a, b; Godefroit, 1994; McGowan & Motani, 2003), but the monophyly of this genus has rarely been questioned (but see Maisch, 2010; Moon, 2017). The current taxonomic instability of *Temnodontosaurus* is notably illustrated by the species '*Ichthyosaurus*' *acutirostris* (Owen, 1840), whose systematic placement remains controversial due to a poorly described holotype (Maisch, 2010). This species has been assigned to *Leptonectes* McGowan, 1996, *Stenopterygius* Jaekel, 1904 and *Temnodontosaurus* in the past (McGowan, 1974; Maisch & Matzke, 2000; McGowan & Motani, 2003; Maisch, 2010) and according to Maisch (2010) it could represent a genus of its own. This is why '*I.*' *acutirostris* needs taxonomic revision. Furthermore, this species currently incorporates '*Ichthyosaurus*' *zetlandicus* (Seeley,1880), even though the differences in cranial architecture between *'I.' zetlandicus* and *'I.' acutirostris* appear clear (compare Seeley, 1880; McGowan, 1974; Chapman & Doyle, 2002).

We provide a complete osteological redescription of the holotype of '*Ichthyosaurus*' *zetlandicus* and we report a new specimen probably attributable to this taxon from the Schistes Carton Formation of Luxembourg. This redescription and the assessment of its phylogenetic placement among Early Jurassic parvipelvians clarifies its systematic position and provides a much-needed step into re-evaluating the systematics of *Temnodontosaurus.*

Institutional abbreviations

CAMSM, Sedgwick Museum of Earth Sciences, Cambridge University, Cambridge, UK; MNHNL, Musée national d'Histoire naturelle de Luxembourg, Luxembourg; NHMUK, Natural History Museum, London, UK; PB, Petrefaktensammlung Banz, Germany; SMNS, Staatliches Museum für Naturkunde, Stuttgart, Germany.

MATERIAL AND METHODS

Spatiotemporal setting of the holotype of '*Ichthyosaurus*' *zetlandicus*

The holotype of '*Ichthyosaurus*' *zetlandicus*, CAMSM J35176, was discovered along the Whitby coastal section in North Yorkshire (UK) (Seeley, 1880; Supporting Information, Fig. S1) and presented to the Sedgwick Museum by the Earl of Zetland, who owned Loftus Alum Quarry (Benton & Taylor, 1984; Benton & Spencer, 1995). The outcrops in this area belong to the Whitby Mudstone Formation (WMF), which are laminated grey to dark grey mudstones (Powell, 2010). CAMSM J35176 is believed to have been found in the Main Alum Shales, a subdivision of the Alum Shale Member where many fossils of marine reptiles have been discovered (Benton & Taylor, 1984). These shales consist of a sequence of poorly laminated dark grey mudstones interbedded by bands of siderite and calcareous concretions and in the upper part by bands of phosphatic nodules (Powell, 2010; Swaby & Lomax, 2020). Biostratigraphically, it belongs to the Bifrons Zone, Middle Toarcian (Hodges *et al.*, 2004).

Spatiotemporal setting of MNHNL TU885

The specimen MNHNL TU885 was found at Schouweiler near Bascharage and Sanem, Grand Duchy of Luxembourg (Fig. 1B), a region well known for its marine reptile fossil richness (Streitz, 1983; Godefroit, 1994; Vincent *et al.*, 2017; Johnson *et al.*, 2019; Fischer *et al.*, 2021). Sediments of this region are Early Toarcian in age and belong to the Schistes Carton unit (Fig. 1A), roughly contemporaneous with the Posidonienschiefer (Germany) and the Whitby Mudstone Formation (England). The black shales that composed these outcrops contain nodular limestone in which many fossils are found preserved three-dimensionally and articulated (Hermoso *et al.*, 2014; Vincent *et al.*, 2017; Johnson *et al.*, 2019). Specimen MNHNL TU885 is likely to have come from one of these nodules (Fig. 1A). Biostratigraphically, the black shales of the Grand Duchy of Luxembourg can be assigned to the Serpentinum Zone, itself subdivided into two subzones: the Elegantum and Falciferum Subzones (Fig. 1A; Hermoso *et al.*, 2014; Vincent *et al.*, 2017; Johnson *et al.*, 2019).

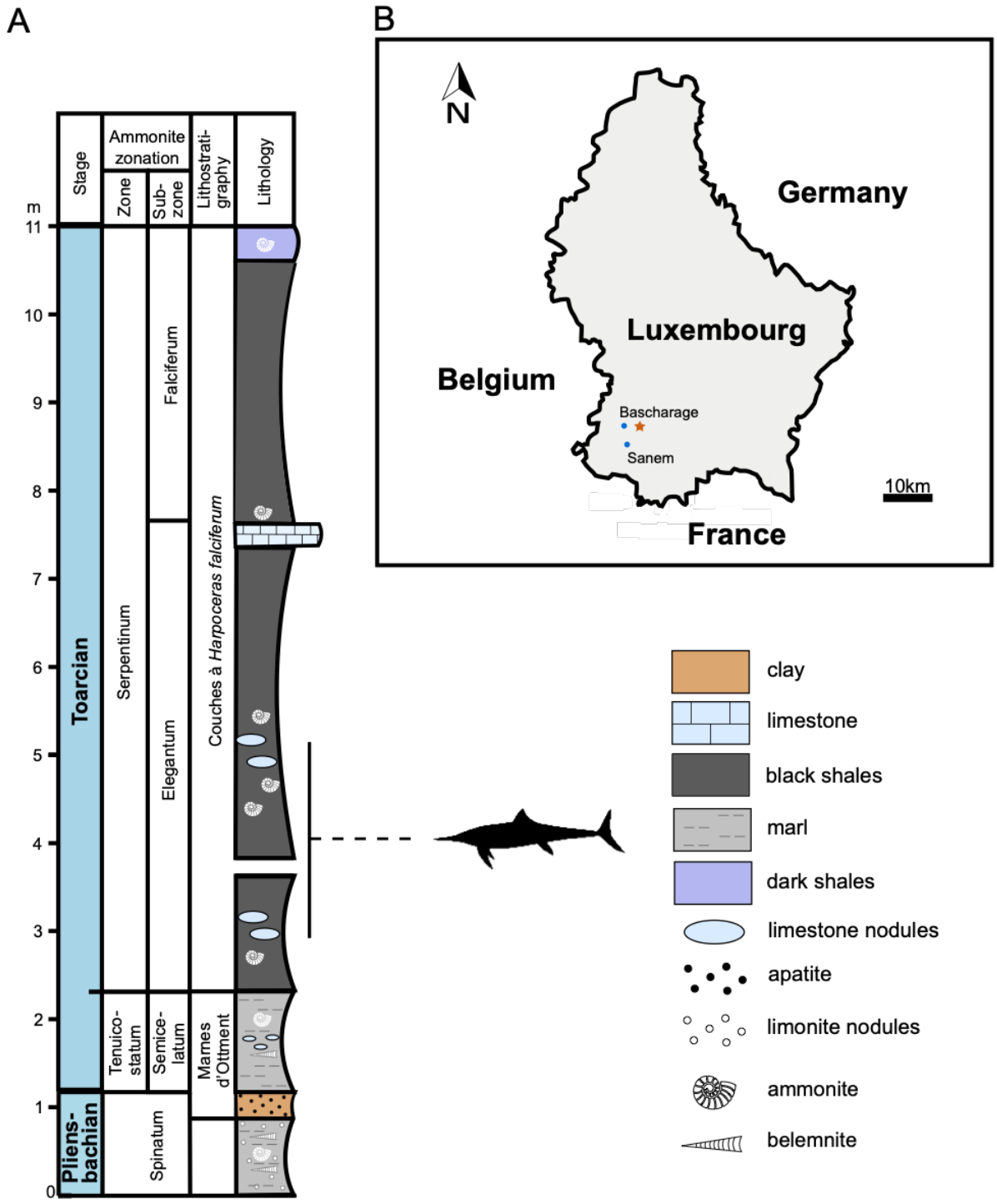

Figure 1. A, schematic log containing the lithology of the Lower Jurassic section of the Grand-Duchy of Luxembourg and the stratigraphic position of MNHNL TU885. B, map of the Grand-Duchy of Luxembourg. The star indicates the discovery site of MNHNL TU885.

Phylogenetic analyses

To assess the phylogenetic position of '*Ichthyosaurus*' *zetlandicus* among early parvipelvians, we scored this taxon based on personal observations on the holotype specimen (CAMSM J35176) in the cladistic data set of Maxwell & Cortés (2020). This cladistic data set derives from the matrix of Maxwell *et al.* (2019), which is itself a modified version of the matrix of Moon (2017). We merged scoring the two Operational Taxonomic Units (OTUs) *Hauffiopteryx typicus* (von Huene, 1931) 'UK' and *Hauffiopteryx typicus* 'German' to obtain a single OTU for this species. We revised the scoring of *Besanosaurus leptorhynchus* Dal Sasso & Pinna, 1996 based on new information provided by Bindellini *et al.* (2021) and we removed *Mikadocephalus gracilirostris* Maisch & Matzke, 1997 because it has been demonstrated to be a synonym of *B. leptorhynchus* (Bindellini *et al.*, 2021). We also revised the scoring of all current species referred to as *Temnodontosaurus*, based on first-hand observations, high-precision 3D models (see below) and the literature (see Supporting Information Text S1). The final matrix is available in the Supporting Information (File S1). We have realized 3D models of the holotype of '*I.*' *zetlandicus* CAMSM J35176, the Luxembourg specimen MNHNL TU885; and two specimens of *T. trigonodon* (Theodori, 1843) (SMNS 17650 and SMNS 50000). These 3D models are available on MorphoSource: https://www.morphosource.org/projects/000351961. We have also used the 3D models of *T. trigonodon* (SMNS 15950) and *T. nuertingensis* (von Huene, 1931) (SMNS 13488) published by Pardo-Pérez *et al.* (2018).

Phylogenetic analyses were carried out within a maximum parsimony and a Bayesian framework. Maximum parsimony analyses were carried out in TNT v.1.5 (Goloboff *et al.*, 2008; Goloboff & Catalano, 2016). In order to minimize the impact of homoplasy, we used the implied weighting method, which reduces the weight of each character proportionally to its homoplasy. We used different values of the concavity constant k (k = 6, k = 9 and k = 12); increasing the K value reduces the penalty applied to homoplastic characters. In a maximum parsimony framework, implied weighting appears to be the method of choice, providing accurate results (Goloboff *et al.*, 2018; Smith, 2019). In TNT, we raised the maximum number of trees to 100 000 and used the New Technology Search (ratchet activated: 200 ratchet iterations; drift activated: ten cycles; five hits; ten trees per replication), to identify islands of most parsimonious trees. We applied the tree bisection-reconnection (TBR) algorithm on the trees recovered by the ratchet analysis to fully explore these islands. In order to identify wildcard taxa, which may cause instability in our most parsimonious trees (MPTs), we used IterPCR (Pol & Escapa, 2009). Therefore, in our MPTs generated with k = 6, we pruned the taxa *Himalayasaurus tibetensis* Dong, 1972, *Palvennia hoybergeti* Druckenmiller *et al*., 2012 and *Pervushovisaurus bannovkensis* Arkhangelsky, 1998, and with k = 9 and k = 12, we pruned *Palvennia hoybergeti* and *Pervushovisaurus bannovkensis.* We also used a symmetric resampling of 33% change probability, which gives the frequency differences for 10 000 replicates to analyse the nodal support of our trees in an implied weighting framework. This resampling method appears to be the most appropriate as it is not distorted by character weight variations (Goloboff *et al.*, 2003). Furthermore, we used the Templeton's parametric test (Templeton, 1983) in TNT to investigate the statistical

difference of topology lengths between our trees and a tree within which there was a positive constraint, testifying the monophyly of *Temnodontosaurus*. Trees were plotted and time scaled *a posteriori* by using an 'equal' method of branch length reconstruction using the strap v.1.4 package (Bell & Lloyd, 2015) in R v.1.3.1093. The stratigraphic congruence was calculated by using the ape v.5.2 (Paradis *et al.*, 2004), geoscale v.2.0 (Bell, 2015) and paleotree v.3.3.25 (Bapst, 2012) packages.

Bayesian inference of topology was conducted in MrBayes (v.3.2.7a; Ronquist *et al.*, 2012) using the CIPRES Science Gateway v.3.3 (Miller *et al.*, 2010). Character states were unweighted and unordered, and state frequencies were defined using a symmetrical Dirchlet hyperprior fixed at infinity which makes all state transitions equally likely. The Mkv model was used for the analysis with a gamma distribution for site rate variation with an exp(1.0) as a hyperprior. We set four runs of four chains, 100 000 000 generations, sampling at every 1000. We also applied a burn-in which discarded the first 25%. Similar parameters have been used in previous Bayesian inferences of ichthyosaurian relationships (Fischer *et al.*, 2016; Moon, 2017). Our script for Bayesian analyses is available in the Supporting Information (File S2).

Systematic Description

Ichthyosauria De Blainville, 1835
Parvipelvia Motani, 1999b
Neoichthyosauria Sander, 2000
Temnodontosauridae McGowan, 1974
Temnodontosaurus Lydekker, 1889
Temnodontosaurus zetlandicus (Seeley, 1880) **comb. nov.**

1880 *Ichthyosaurus zetlandicus* – Seeley
1881 *Ichthyosaurus longifrons* – Owen
1889b *Ichthyosaurus zetlandicus* – Lydekker
1890 *Ichthyosaurus zetlandicus* – Woodward & Sherborn
1891 *Ichthyosaurus zetlandicus* – Fraas
1922 *Stenopterygius zetlandicus* – Huene
1925 *Stenopterygius zetlandicus* – Hauff
1974 *Stenopterygius acutirostris* – McGowan
1997 *Temnodontosaurus acutirostris* – Maisch & Hungerbühler
2000 *Temnodontosaurus acutirostris* – Maisch & Matzke
2003 *Temnodontosaurus acutirostris* – McGowan
2010 '*Ichthyosaurus*' *acutirostris* – Maisch
2019 *?Temnodontosaurus acutirostris* – Lomax

Holotype, stratum typicum and locus typicus: CAMSM J35176, a three-dimensionally preserved skull missing the mandible and the anterior third of the rostrum, from the Whitby Mudstone Formation, Lower Toarcian, likely from the Loftus Alum Quarry close to Whitby, Yorkshire, UK.

Emended diagnosis: *Temnodontosaurus zetlandicus* is characterized by the following unique combination of unusual features among early neoichthyosaurians: a digitate anterior end of the jugal which covers the maxilla, externally separates the maxilla and the lacrimal and slightly overlaps the subnarial process of the premaxilla (shared with *T. nuertingensis* and *T. trigonodon*); bifurcated posterior end of the jugal, resulting in the separation of the ascending process and a smaller anteroventrally oriented process (shared with *T. trigonodon*); presence of a prom ainent mediolaterally oriented ridge which forms the anterior margin of the supratemporal fenestra (shared with *T.*

trigonodon); slender projection of the supratemporal which covers the postfrontal dorsally and does not reach the anterior margin of the supratemporal fenestra (shared with *T. trigonodon*); presence of a prominent sagittal crest on the parietal and a slender parietal fork that partially overlaps the frontal (shared with *T. trigonodon*); absence of a postnarial descending process; presence of two posterior processes of the nasal, the lateral ending by an interdigitated suture, overlapping the anterior edge of the postfrontal which thus is bifurcated and adopts a V-shape, resulting in the separation of a medial and an anterodorsal process; and dorsal region of the lacrimal less extended than in *T. trigonodon* and marked by a notch.

Comparative description of the holotype CAMSM J35176*:* First described by Seeley in 1880, this specimen (Figs 2–4) is a cranium measuring 720 mm long; the mandible is not preserved. The end of the rostrum appears to have been broken off and we estimate the cranium and the snout to be respectively 990 mm and 680 mm long *in vivo* by prolonging the lateral edges of the premaxilla. The rostrum is straight, unlike in '*Ichthyosaurus*' *acutirostris* (Owen, 1865–1881) even if this feature could be due to the taphonomic flattening. Some badly preserved teeth are located on the premaxilla and the maxilla (Fig. 2) and are marked by striations on the crown. The dorsal part of the basicranium is poorly preserved (Fig. 4); the posterior edge of the parietals, the supraoccipital, the exoccipitals and the dorsal part of the basioccipital are missing. Aside from these elements, the skull is well preserved in three dimensions. All elements of the braincase are made of finished bone and therefore do not have a rugose texture, especially the basioccipital for which the condyle is as smooth as the extracondylar area and for which the opisthotic facets are protruding. This suggests an adult or at least subadult ontogenetic stage for CAMSM J35176 (Miedema & Maxwell, 2019).

The **premaxilla** is markedly elongated and not fully preserved (Figs 2, 3). The medial suture is clearly visible. Laterally, the premaxilla is marked by the presence of the premaxillary fossa and forms the supranarial and subnarial processes, as in other early parvipelvians even if this character may be variable in *Hauffiopteryx* (Maxwell & Cortés, 2020). The supranarial process forms approximately half of the dorsal margin of the naris as in *Temnodontosaurus eurycephalus* (McGowan, 1974) and in *Temnodontosaurus trigonodon* (Maisch, 1998b). The suture of the supranarial process with the nasal is crenulated while the posterior extremity of subnarial process contacts the anterior end of the jugal as in *T. trigonodon* (Maisch, 1998b). The subnarial process also contacts the anterior edge of the lacrimal. Some badly preserved tooth roots are located on its ventral surface but cannot be precisely described.

The **maxilla** is dorsoventrally low, slender and extends anteriorly as far as the nasal (Fig. 2). This particular feature is typical of *Temnodontosaurus* (Maisch & Hungerbühler, 1997; Martin *et al.*, 2012; Swaby & Lomax, 2020) among early parvipelvians. The maxilla of *T. zetlandicus* seems to have a comparable size to that of '*I.*' *acutirostris* (Figs 2, 8) and lower than in *T. nuertingensis* which has a higher maxilla (Maisch & Hungerbühler, 1997). Moreover, the maxilla lacks a narial process and does not participate in the ventral margin of the external naris. The posterior part of the maxilla is covered by the jugal, thus excluding an external contact with the

lacrimal as in *T. trigonodon* (Maisch, 1998b; Pardo- Pérez *et al.*, 2018).

The **external naris** has a typical droplet shape (Fig. 2) and is larger than in *Ichthyosaurus* De la Beche & Conybeare, 1821 (Lomax & Massare, 2016) and *Leptonectes* (Maisch & Matzke, 2003; McGowan, 1989). The anterior extremity is thinner than the posterior border which is exclusively formed by a shallow notch of the lacrimal.

The **nasal** is wide and robust, forming a fairly large portion of the dorsal region (Fig. 3A, B). The anterior part of the nasal cannot be precisely distinguished due to the reconstructed area but appears to end abruptly as in *Temnodontosaurus crassimanus* (Blake, 1876) (Swaby & Lomax, 2020), *T. nuertingensis* (Maisch & Hungerbühler, 1997) and *T. trigonodon* (Pardo-Pérez *et al.*, 2018). The posterior half of the two nasals form a well demarcated internasal cavity. Posteriorly, the nasal forms two processes (one medial and one lateral) overlapping the anterior part of the postfrontal (Fig. 3A, B). The medial process has no digitation and exclusively contacts the postfrontal medially. Therefore, there is no nasal-parietal contact, at least externally. The lateral process is located more laterally and marked by a three-finger digitation. Laterally, the nasal forms approximately half of the dorsal margin of the external naris and a lateral wing is absent, as is the case in all early parvipelvians with the exception of *Leptonectes tenuirostris* (Conybeare, 1822) (Maisch & Matzke, 2003; Massare *et al.*, 2021) and *Stenopterygius aaleniensis* Maxwell *et al.*, 2012 (Massare *et al.*, 2021). Furthermore, the nasal does not make a postnarial descending process, unlike *Temnodontosaurus platyodon* (Conybeare, 1822) (e.g. NHMUK R1158), *T. nuertingensis* (Maisch, 1997; Massare *et al.*, 2021) and *T. trigonodon* (Maisch, 1998b; Maisch & Hungerbühler, 2001). The **lacrimal** has a broad hatchet shape, as is usual for ichthyosaurians (Fig. 2). The posterior margin participates to the anterior and anteroventral margins of the orbit while the anterior margin also forms the posterior margin of the external naris without forming a rounded bulge or a prominent process within the naris, as can be seen in many specimens of *Temnodontosaurus* (Massare *et al.*, 2021). The lacrimal is marked by a notch on the dorsal edge unlike in *Temnodontosaurus platyodon* (Godefroit, 1993a), *Leptonectes* spp. (Maisch & Matzke, 2003), *Suevoleviathan* Maisch, 1998 spp. (Maisch, 2001), *Ichthyosaurus* spp. (Lomax & Massare, 2016), *Protoichthyosaurus* Appleby, 1979 (Lomax & Massare, 2018) and *Stenopterygius* spp. (Caine & Benton, 2011) and is not as extended dorsally as in *T. trigonodon* where the dorsal notch is also absent (Maisch, 1998b; Maisch & Hungerbühler, 2001; Pardo- Pérez *et al.*, 2018). Moreover, the suture with the prefrontal is slightly crenulated. The ventral edge is more convex and entirely in contact with the jugal.

The **lacrimal** has a broad hatchet shape, as is usual for ichthyosaurians (Fig. 2). The posterior margin participates to the anterior and anteroventral margins of the orbit while the anterior margin also forms the posterior margin of the external naris without forming a as can be seen in many specimens of *Temnodontosaurus* (Massare *et al.*, 2021). The lacrimal is marked by a notch on the dorsal edge unlike in *Temnodontosaurus platyodon* (Godefroit, 1993a), *Leptonectes* spp. (Maisch & Matzke, 2003), *Suevoleviathan* Maisch, 1998 spp. (Maisch, 2001), *Ichthyosaurus* spp. (Lomax & Massare, 2016), *Protoichthyosaurus* Appleby, 1979 (Lomax & Massare, 2018) and

Stenopterygius spp. (Caine & Benton, 2011) and is not as extended dorsally as in *T. trigonodon* where the dorsal notch is also absent (Maisch, 1998b; Maisch & Hungerbühler, 2001; Pardo- Pérez *et al.*, 2018). Moreover, the suture with the prefrontal is slightly crenulated. The ventral edge is more convex and entirely in contact with the jugal.

The **prefrontal** accounts for approximatively one third of the dorsal margin of the orbit (Figs 2, 3A, B). The anterior extremity contacts the lacrimal and this suture appears to be weakly crenulated. The prefrontal does not form a narial process, and hence does not participate to the rim of the external naris, a feature that is shared with most early parvipelvians with the exception of *Hauffiopteryx* Maisch, 2008 (Maxwell & Cortés, 2020). The prefrontal is not dorsomedially extended and does not contact the frontal or the parietal, unlike in *Leptonectes* (Maisch & Matzke, 2003), *Stenopterygius* (Maxwell *et al.*, 2012) and *Hauffiopteryx* (Maxwell & Cortés, 2020). The suture with the postfrontal seems to be slightly interdigitated.

Externally, the **frontal** is a small lanceolate bone that forms a narrow triangular process anteriorly (Fig. 3A, B). The posterior part is wider and is covered by the slender parietal fork, as in *T. trigonodon* (Maisch, 1998b) and therefore differs from *Hauffiopteryx* (Maxwell & Cortés, 2020), *Ichthyosaurus* (McGowan, 1973), *Leptonectes* (Maisch & Matzke, 2003; Vincent *et al.*, 2014), *Protoichthyosaurus* (Lomax *et al.*, 2020) and *Stenopterygius* (Maxwell *et al.*, 2012) in which the parietal anterior termination is broader. The frontal only participates in the formation of the anterior margin of the parietal foramen as in *T. trigonodon* (Maisch, 1998b), but unlike in *Hauffiopteryx* (Maxwell & Cortés, 2020), *Leptonectes* (Maisch & Matzke, 2003), *Protoichthyosaurus* (Lomax *et al.*, 2020), *Stenopterygius* (Maxwell *et al.*, 2012) or *Wahlisaurus* Lomax, 2016, in which frontals also form the lateral margin of the parietal foramen. Laterally, the frontal does not reach the supratemporal fenestra, as in all early parvipelvians (McGowan, 1973; Maisch & Matzke, 2003; Maxwell *et al.*, 2012; Marek *et al.*, 2015; Lomax, 2016; Maxwell & Cortés, 2020).

The **jugal** is slender and forms the ventral and posteroventral margins of the orbit (Fig. 2). The posterior extremity of the jugal contacts the postorbital and the quadratojugal, unlike in *Hauffiopteryx* (Maxwell & Cortés, 2020) and *Stenopterygius* (Maisch, 2008). This extremity appears bifurcated, resulting in the separation of the ascending process and a small anteroventrally oriented process (Fig. 2C, D). Such a bifurcation is also found in *T. trigonodon* and could be due to an anteroventral process of the quadratojugal (Maisch & Hungerbühler, 2001). However, the ascending process is broader in *T. trigonodon* (Maisch & Hungerbühler, 2001; Pardo-Pérez *et al.*, 2018). The anterior extremity of the jugal is digitated, contacting the subnarial process of the premaxilla and covering the posterior part of the maxilla (Fig. 2). This contact between the jugal and the premaxilla is also present in *T. trigonodon* (Maisch, 1998b; Fig. 12) and in *T. nuertingensis* (Maisch & Hungerbühler, 1997), but not in other early parvipelvians.

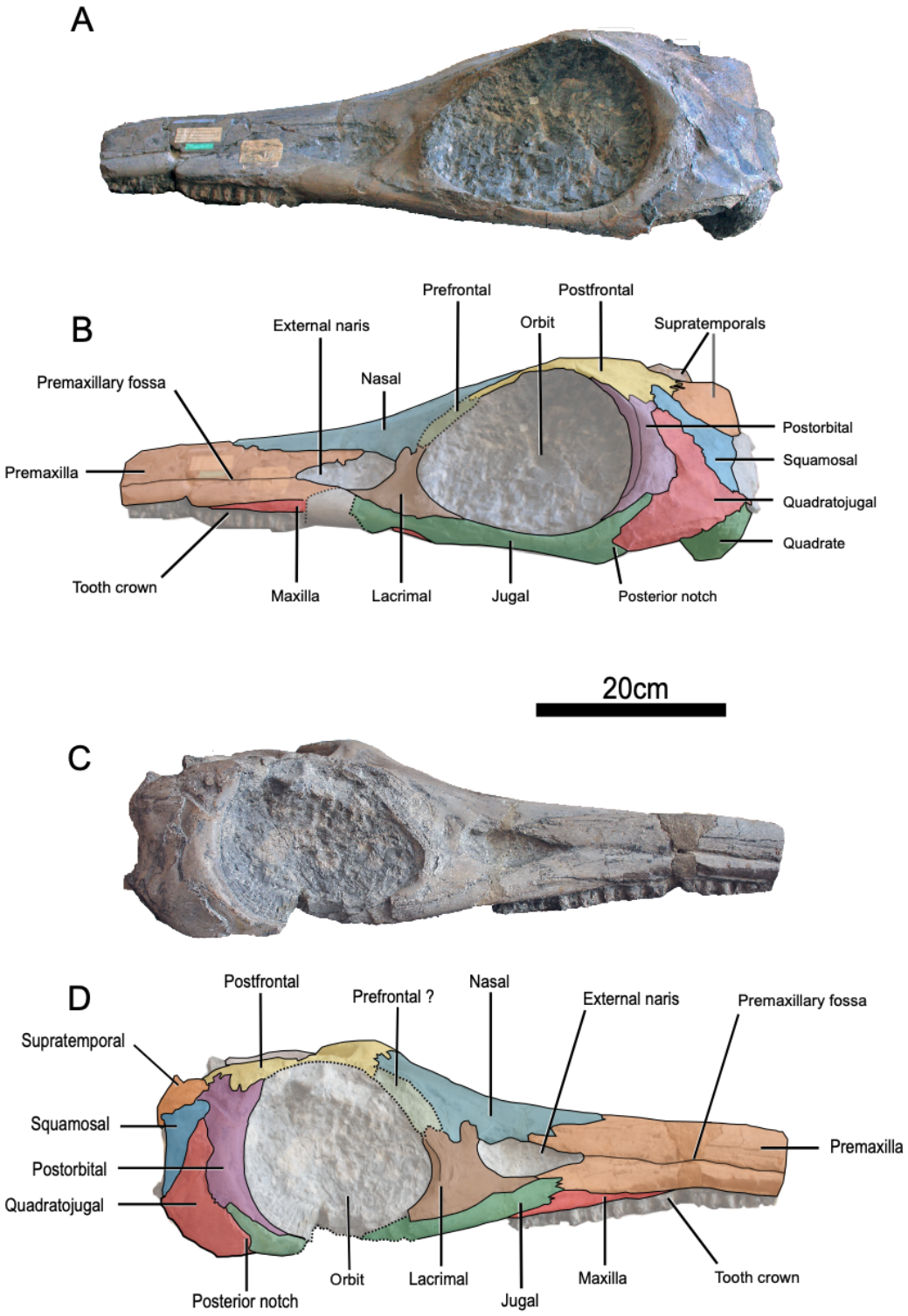

Figure 3. Photograph and interpretation of the holotype of *Temnodontosaurus zetlandicus* comb. nov. (CAMSM J35176). A, B, in left lateral view. C, D, in right lateral view.

The **quadratojugal** appears to form the frame of the postorbital region and is well exposed (Fig. 2) as in *Ichthyosaurus* (Lomax & Massare, 2016) and *Temnodontosaurus* (McGowan, 1974; Godefroit, 1993a; Maisch & Hungerbühler, 2001) and unlike in *Hauffiopteryx* (Maxwell & Cortés, 2020) and *Stenopterygius* (Godefroit, 1993b; Maisch, 2008). The quadratojugal is wide, especially the ventral part where it extends to the level of the posterior digitation of the jugal (as in *T. trigonodon*; Maisch & Hungerbühler, 2001). The quadratojugal forms a large dorsal process, which nearly reaches the dorsal margin of the squamosal (Fig. 2). The articulation surface with the quadrate is strongly concave medioventrally. The anterior edge the quadratojugal seems to slightly cover the posterior margin of the postorbital. Posterodorsally, the quadratojugal contacts the squamosal along a relatively smooth suture. The postorbital region is large compared to the orbit but less than in *T. trigonodon* even if this ratio looks variable within the species (ratio length of the postorbital region to length of the orbit: ~0.5 for *T. zetlandicus* vs. ~0.6–1.0 for *T. trigonodon*; see Supporting Information, Table S1).

The **squamosal** is a relatively large triangular element within the postorbital region (Fig. 2) and has a morphology similar to that of *T. trigonodon* (Maisch & Hungerbühler, 2001). The posteroventral process of the squamosal is long and reaches the articulation between the quadratojugal and the condyle of the quadrate. Laterally, the suture with the quadratojugal is well extended and dorsally, the squamosal contacts the supratemporal and the postfrontal by an anterodorsal process (Fig. 2).

The crescent-shaped **postorbital** forms the posterior margin of the orbit (Fig. 2). Dorsally, the facet with the postfrontal is reduced in comparison to *Suevoleviathan* (Maisch, 2001) and ventrally, the postorbital contacts the jugal. The orbital crest is not prominent on postorbital, thus resulting in a lack of clear delimitation of the part involved in the formation of the orbit and the part forming the postorbital region. The postorbital thins dorsally and ventrally, buttressing the postfrontal and the dorsal margin of the jugal. Posteriorly, the postorbital contacts the quadratojugal and seems to be slightly overlapped by this element.

The **parietals** are relatively well preserved except at their posterior part and have a curved aspect (Fig. 3A, B). The anterior extremity of the parietal is marked by a slender parietal fork that covers the posterior part of the frontal as in *T. trigonodon* (Fig. 12, B, C; Maisch, 1998b). As a result, the posterior and lateral margins of the parietal foramen are formed externally by this element and this foramen is nearly enclosed by the parietals except at its anterior edge (Fig. 3A, B, 7). This strongly contrasts with *Hauffiopteryx* (Marek *et al.*, 2015), *Stenopterygius* (Maxwell *et al.*, 2012) and *Wahlisaurus* (Lomax, 2016), where the parietal foramen is nearly completely enclosed by the frontals. The interparietal suture is surrounded by a prominent parasagittal ridge (Fig. 3A, B), which is present on both elements, thus forming a paired structure as in *T. trigonodon* (Fig. 12). This ridge becomes thinner and flatter posteriorly and ends anteriorly at the posterior edge of the parietal foramen. Dorsally, the suture between the parietal and the supratemporal adopts a sinusoidal configuration.

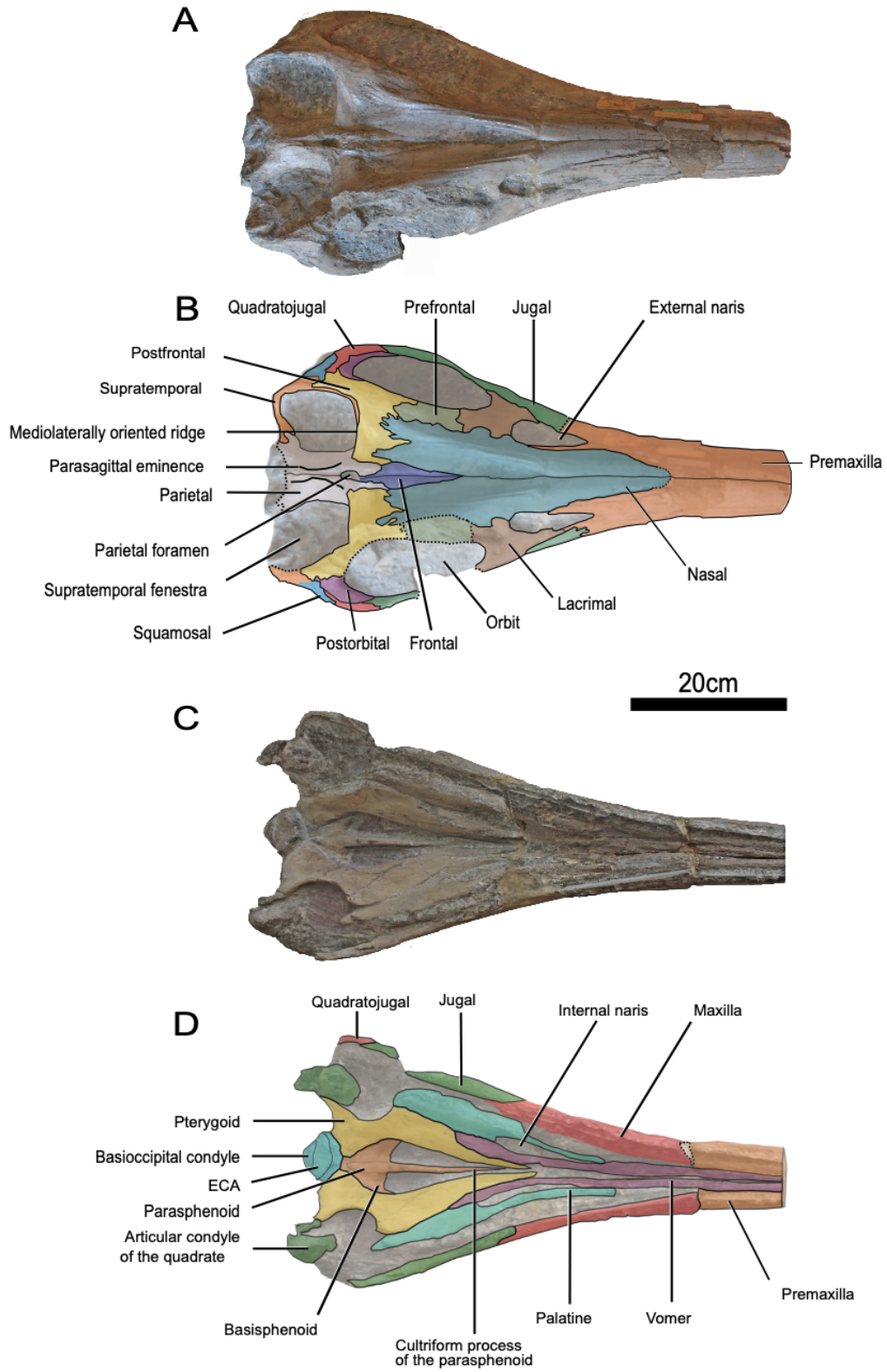

Figure 3. Photograph and interpretation of the holotype of *Temnodontosaurus zetlandicus* comb. nov. (CAMSM J35176). A, B, in dorsal view. C, D, in ventral view. Abbreviation: ECA, extracondylar area of the basioccipital.

The **supratemporal** is a strongly curved bone (Fig. 3A, B). It forms the posterior and lateral margins of the supratemporal fenestra, forming an elongated anteromedial process that covers the postfrontal laterally and reaches the anterior ridge of the supratemporal fenestra (Fig. 3A, B) formed by the dorsal part of the postfrontal (see below) as in *T. trigonodon* (Fig. 12). The suture with the postfrontal is digitated and the contact with the squamosal is extensive (Fig. 2). The descending process of the supratemporal forms the lateral margin of the braincase, where it contacts the occipital lamella of the quadrate (Fig. 4).

The left postfrontal is completely preserved while the anterolateral portion of the right one is damaged (Figs 2, 3A, B). The **postfrontal** is an extensive structure participating in the dorsal and postorbital regions of the cranium. Anteriorly, this element is partially covered by the posterior processes of the nasal, giving it a V-shape dorsally, resulting in the bifurcation of a medial and a lateral process, which it is not seen in any early parvipelvians (Maisch, 1998b; Maisch & Matzke, 2003; Maxwell *et al.*, 2012; Vincent *et al.*, 2014; Marek *et al.*, 2015; Lomax, 2016; Lomax & Massare, 2016; Lomax *et al.*, 2020; Maxwell & Cortés, 2020). The suture with the prefrontal is not well preserved but appears undulated. The postfrontal forms the entire anterior margin of the supratemporal fenestra where this element forms an extensive mediolaterally oriented ridge (Fig. 3A, B, 7). This unusual structure is actually shared with *T. trigonodon* (Fig. 12). A short ridge is also present in *Protoichthyosaurus prostaxalis* Appleby, 1979 (Lomax & Massare, 2018). However, this postfrontal ridge appears shorter than in *T. zetlandicus* (medially vanished around mid-supratemporal fenestra width) and also appears to be oriented along the anteromedial-posterolateral axis whereas this ridge is mediolaterally oriented in *T. zetlandicus* (Figs 3A, B). Apart from these three species, the presence of a postfrontal ridge which forms the anterior edge of the supratemporal fenestra is absent in all other early parvipelvians (McGowan, 1973; Maisch, 1998a; Maisch & Matzke, 2003; Maxwell *et al.*, 2012; Vincent *et al.*, 2014; Marek *et al.*, 2015; Lomax, 2016; Lomax & Massare, 2016; 2012; *al.*, 2020; Maxwell & Cortés, 2020).

The **basioccipital** is partially preserved, having its dorsal part damaged (Fig. 4). Thus, its contribution to the foramen magnum cannot be characterized. The condyle is prominent and is clearly separated from the extracondylar area, a character shared by members of *Temnodontosaurus* (Swaby & Lomax, 2020) and more generally, non-ophthalmosaurid parvipelvians (Motani, 1999b; Fischer *et al.*, 2012) and the notochordal pit is located on the centre of the condyle. The extracondylar area is slightly expanded laterally and seems to be well developed ventrally and marked by the presence of a basal tubera, thus being saddle-shaped ventrally, unlike in *Stenopterygius quadriscissus* (Quenstedt, 1856) (Miedema & Maxwell, 2019) and *Chacaicosaurus* Fernández, 1994. The protrusion of the opisthotic and stapedial facets is discernible, resulting in concave and well-delimited facets.

The **stapes** possesses a robust shaft that is only slightly waisted (Fig. 4). The proximal head seems to be massive as in *T. trigonodon* (Maisch, 2002), *Eurhinosaurus longirostris* (Mantell, 1851) (e.g. SMNS 18648), *Hauffiopteryx* (Marek *et al.*, 2015) and *Stenopterygius quadriscissus* (Miedema & Maxwell, 2019) but unlike in *Ichthyosaurus* (McGowan, 1973), *Protoichthyosaurus* (Lomax *et al.*, 2019) and

Temnodontosaurus azerguensis Martin *et al.*, 2012. The medial surface of the proximal head is concave, matching the slightly convex corresponding facet on the basioccipital. The distal facet for articulation with the quadrate is elliptic and weakly expanded with respect to the shaft.

Both **quadrates** are poorly preserved (Fig. 4). The dorsal suture with the supratemporal and the laterally to the right quadrate with the stapes is nevertheless visible. The condyle, located at the ventrolateral end of the posterior face, is better preserved and massive. With a reniform aspect, the dorsolateral edge adopts a shape complementary to the contact facet of the quadratojugal and is therefore largely convex. The ventral edge of the condyle is more concave and would serve to accommodate the surangular which is not preserved. The ventromedial edge contacts the quadrate wing of the pterygoid.

The **pterygoid** is a long robust element, markedly constricted at mid-length (Fig. 3C, D), as is usually the case in parvipelvians (McGowan, 1973). The markedly concave borders of the pterygoid delimit the suborbital fenestra laterally and the large interpterygoid vacuity. The narrow palatine ramus of the pterygoid sharply terminates medially of the internal naris. Laterally, the pterygoid contacts the palatine, and also the vomer more anteriorly by a long straight suture, and there is no postpalatine process. The pterygoid expands posteriorly, forming two horizontal lamellae in the region of the quadrate ramus. The larger lateral lamella contacts the condyle of the quadrate and the smaller medial one contacts the ventral extremity of the extracondylar area of the basioccipital.

The **palatine** is fairly elongated and forms posteriorly the anterior margin of the suborbital fenestra (Fig. 3C, D). Its concave medial edge forms the lateral margin of the internal naris. The anterior half of the palatine becomes considerably thinner and its extremity ends by a junction with the vomer.

The **vomer** is also elongated; its widest portion is set posteriorly, where it forms the medial margin of the internal naris (Fig. 3C, D). The vomer extends anteriorly as a slit-like process, contacting the premaxilla and the palatine. Posteriorly the vomer is not well extended as in *T. nuertingensis* and almost excludes a contact between the pterygoid and the palatine (Maisch & Hungerbühler, 1997).

The **basisphenoid** appears crescent shaped in ventral view as its anterior edge is concave (Fig. 3C, D). The posterior surface in contact with the basioccipital is hidden laterally by the pterygoids, as well as the basipterygoidal processes laterally. The basisphenoid is medially crossed throughout its entire length by the parasphenoid; even though the carotid foramina is not visible, this extension of the parasphenoid indicates that this foramen was paired like all members of *Temnodontosaurus* (Fraas, 1913; von Huene, 1931; Godefroit, 1993a; Maisch & Matzke, 2000; Maisch, 2002; Martin *et al.*, 2012).

The **parasphenoid** forms a relatively robust cultriform process (Fig. 3C, D). The parasphenoid extends from the posterior end of the basisphenoid to approximately half the length of the palate region but does not reach the interpterygoidal suture.

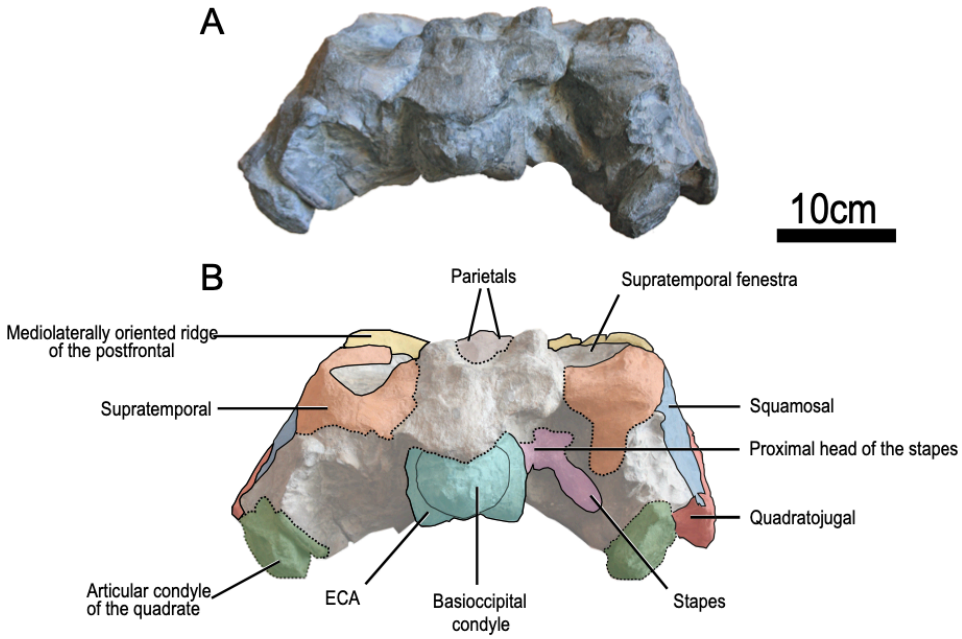

Figure 4. Photograph and interpretation of the holotype of *Temnodontosaurus zetlandicus* comb. nov. (CAMSM J35176). A, B, Basicranium in posterior view. Abbreviation: ECA, extracondylar area of the basioccipital.

Temnodontosaurus cf. *zetlandicus*

Referred specimen: MNHNL TU885, a partial skull from the Schistes Carton Formation, Lower Toarcian, Schouweiler, Grand Duchy of Luxembourg.

Comparative description of MNHNL TU885*:* The specimen MNHNL TU885 is, as preserved, 383 mm long and consists of a cranium lacking the snout and a fragmentary surangular (Figs 5, 6). Due to its preservation state, the orbits and temporal fenestrae are not fully delimited, and the right vomer and the left palatine have been slightly displaced (Fig. 6A, B). The sutures between the nasals, frontals, right prefrontal and postfrontals are often difficult to discern (Fig. 5C, D). The parietal foramen is entirely preserved and appears unusually large, with a markedly raised rim; it is presently unclear whether this condition is pathological or not, as the parietal foramen is not located on the cranial midline. The postorbital region isonly preserved on the left side and is anteroposteriorly long (Fig. 5A, B), measuring 99 mmThe postorbital region is only preserved on the left side and is anteroposteriorly long (Fig. 5A, B), measuring 99 mm. The basicranium is completely preserved (Fig. 6C, D), only lacking the left opisthotic. Hereafter, we compare salient features of MNHNL TU885 with early neoichthyosaurians. This specimen shares many features with early neoichthyosaurians such as a frontal without a temporal process, a supraoccipital with a shallow ventral notch, a robust stapes with a prominent proximal head, a stout opisthotic with a short paroccipital process, a basioccipital with a well-demarcated extracondylar area, which is ventrally saddle-shaped and marked by the presence of a basal tubera, and a paired carotid foramen as suggested by the morphology of the parasphenoid, even if the posterior part mostly seems to be broken (McGowan, 1973; Fischer *et al.*, 2011; Martin *et al.*,

2012; Marek *et al.*, 2015; Moon & Kirton, 2016; Lomax *et al.*, 2019; Miedema & Maxwell, 2019). In posterior view (Fig. 6C, D), the quadrate is a robust and large element that has a straight occipital lamella unlike *T. azerguensis* (Martin *et al.*, 2012) and *T. crassimanus* (Swaby & Lomax, 2020) and with a massive and well-developed condyle as in species currently referred to as *Temnodontosaurus* for which the quadrate is preserved, with the exception of *T. azerguensis* (Martin *et al.*, 2012). The postorbital region is well developed with a long, extensive quadratojugal, as in *Temnodontosaurus* spp. (McGowan, 1974, 1994; Maisch & Hungerbühler, 2001; Swaby & Lomax, 2020) but unlike in other Early Jurassic parvipelvians (Maisch, 2001, 2008; Maisch & Matzke, 2003; Lomax & Massare, 2016; Maxwell & Cortés, 2020). The contribution of the supraoccipital to the dorsal margin of the foramen magnum is limited and nearly absent, as in *Temnodontosaurus* (Maisch, 2002). The frontal has a reduced, lanceolate dorsal exposure and forms the anterior margin of the parietal foramen, as in *T.zetlandicus* and *T. trigonodon* (Maisch, 1998b). For all of these reasons, MNHNL TU885 is clearly assignable to *Temnodontosaurus*. The skull roof of MNHNL TU885 shares many similarities with that of *T. zetlandicus* (Fig. 7), such as: (1) the bifurcated posterior processes of the nasal which partially covers the postfrontal which anteriorly appears in the medial and anterolateral processes; (2) the presence of a prominent mediolaterally oriented ridge on the postfrontal which forms the anterior margin of the supratemporal fenestra; and (3) a lanceolate frontal posteriorly covered by a slender forked process of the parietal. The skull roof of MNHNL TU885 also resembles that of *T. trigonodon*, but the presence of the bifurcated posterior processes of the nasal markedly differs from *T. trigonodon* (Maisch, 1998b). MNHNL TU885 is also similar in size and in cranial proportions to *T. zetlandicus* (see

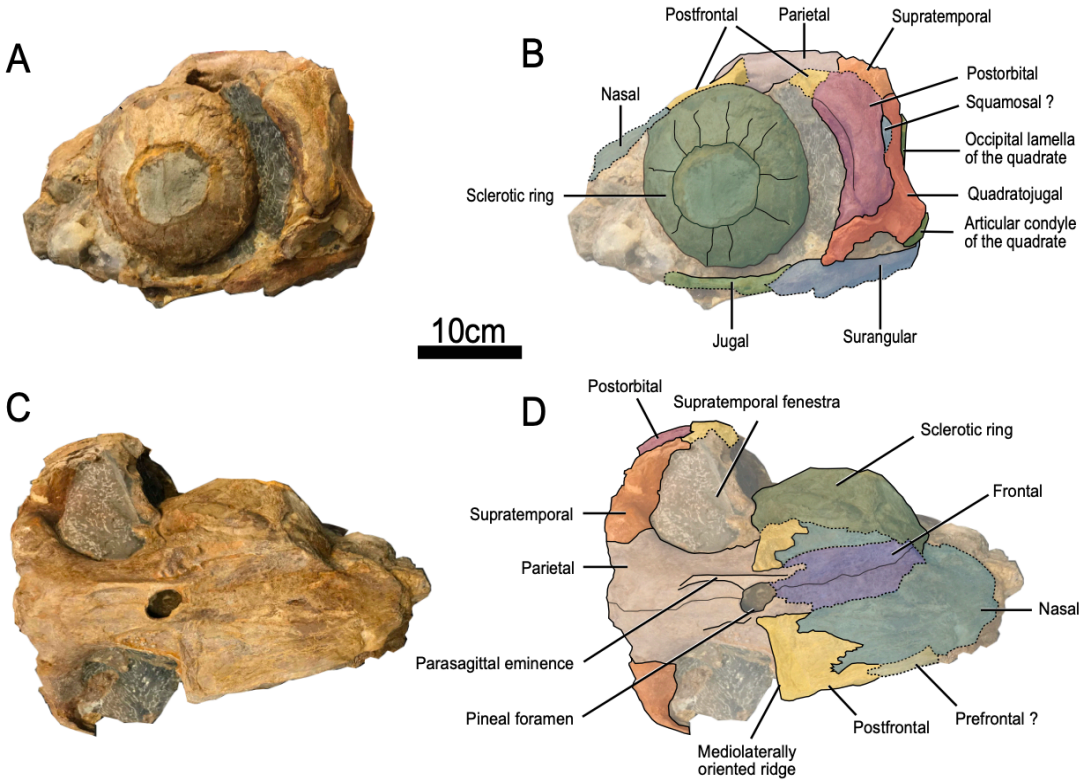

Figure 5. Photograph and interpretation of the specimen MNHNL TU885 *Temnodontosaurus* cf. *zetlandicus* A, B, in right lateral view. C, D, in dorsal view.

Table 1) and is here referred to as *T.* cf. *zetlandicus*.

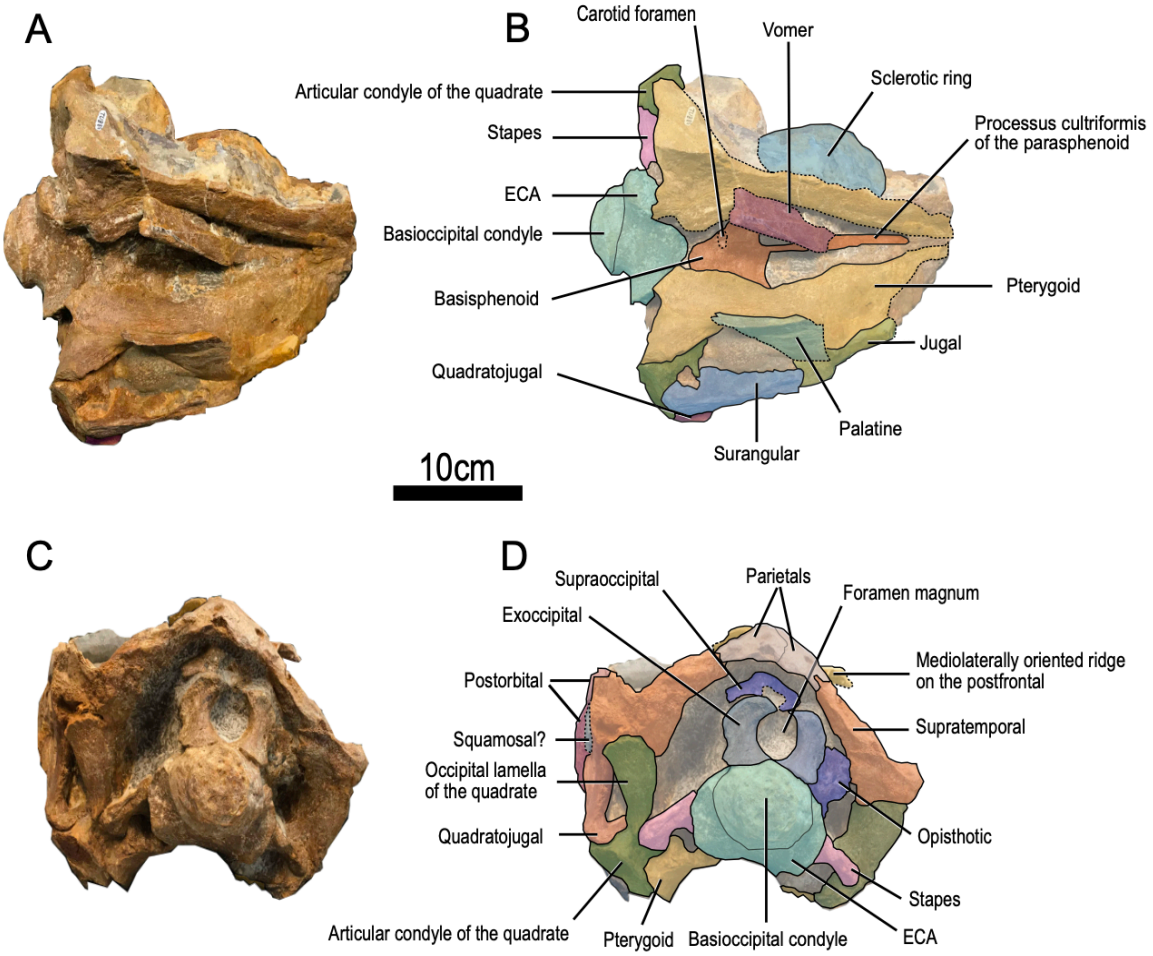

Figure 6. Photograph and interpretation of the specimen MNHNL TU885 *Temnodontosaurus* cf. *zetlandicus* A, B, palate in ventral view. C, D, Basicranium in posterior view. Abbreviation: ECA, extracondylar area of the basioccipital.

Table 1. Measurements (anteroposterior length, diameter, dorsoventral height, mediolateral width) of *Temnodontosaurus zetlandicus* comb. nov. (holotype CAMSM J35176) and *Temnodontosaurus* cf. *zetlandicus* (MNHNL TU885)

Measurements	CAMSM J35176	MNHNL TU885
Length of the skull (estimation)	990	—
Length of the rostrum (estimation)	680	—
Length of the pre-naris rostrum (estimation)	544	—
Height of the left orbit	160	—

Length of the left orbit	195	—
Height of the right orbit	164	—
Length of the right orbit	201	—
Height of the left sclerotic ring	—	165
Length of the left sclerotic ring	—	159
Length of the left UTF	165	—
Length of the right UTF	~149	147
Length of the left naris	109	—
Length of the right naris	112	—
Length of the parietal foramen28	30	28
Width of the parietal foramen	10	20
Length of the left postorbital region	106	895
Length of the right postorbital region	95	—
Length of the parietal	173	152
Length of the frontal	125	~120
Height of the basioccipital	—	102
Width of the basioccipital	90	103
Height of the basioccipital condyle	—	61
Width of the basioccipital condyle	66	78

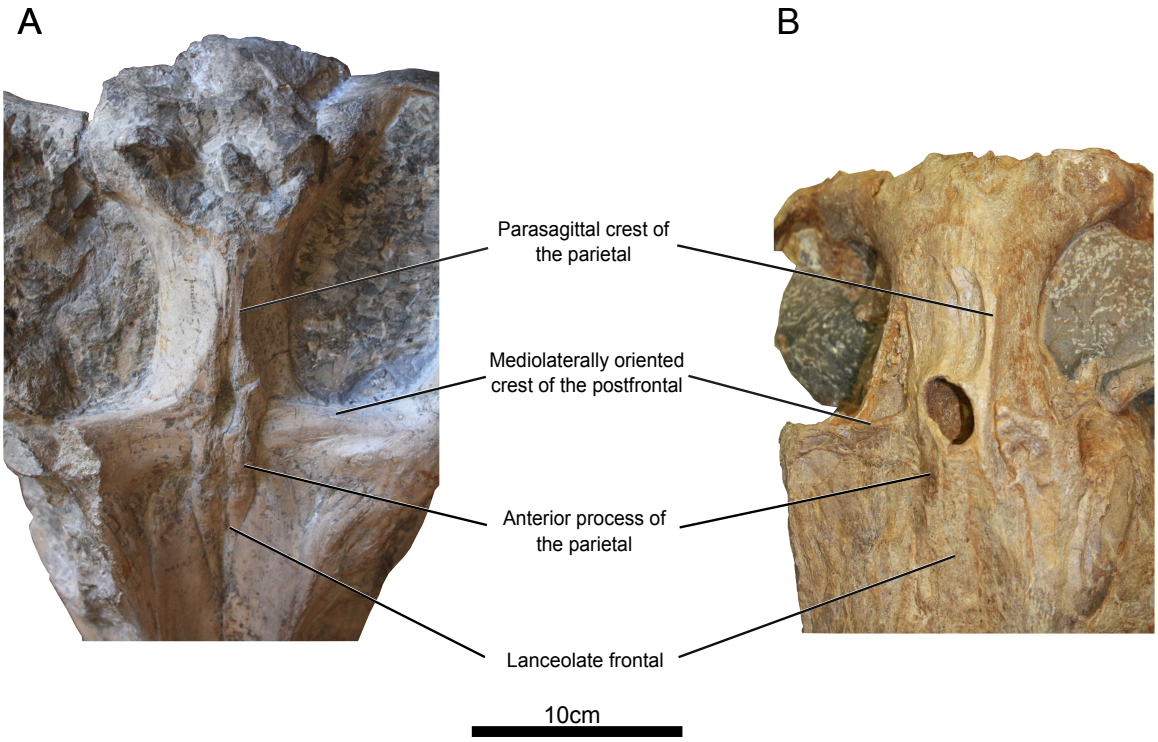

Figure 7. Braincase comparison of the holotype of *Temnodontosaurus zetlandicus* comb. nov. (CAMSM J35176) (A) and the referred specimen of *Temnodontosaurus* cf. *zetlandicus* (MNHNL TU885) (B).

species inquirenda
Ichthyosaurus acutirostris Owen, 1840

In the past, *T. zetlandicus* has been regarded as a junior synonym of '*Ichthyosaurus*' *acutirostris* mainly because both came from the Lower Toarcian of Whitby (UK), without considering differences in cranial shape (McGowan, 1974; McGowan & Motani, 2003; Maisch, 2010). The current taxonomic placement of '*I.*' *acutirostris* is still controversial and has widely fluctuated overtime as this species has been classified in numerous genera (McGowan, 1974; Maisch & Matzke, 2000; McGowan & Motani, 2003; Maisch, 2010). According to Maisch (2010), this species might represent a novel genus of Early Jurassic ichthyosaurian. Considering that the referred material from Whitby requires a complete revision, possibly representing a variety of taxa (Maisch, 2010), focusing on the holotype seems adequate for the time being. However, this holotype (NHMUK PV OR 14553) (Fig. 8) was thought to be lost but finally relocated in the ichthyosaur collections about 20 years ago (Chapman & Doyle, 2002; Lomax, 2019), in a damaged state since the anterior part of the rostrum and the basal part of the right forefin are now missing. Even more problematic, the specimen is *de facto* unavailable for an undefined period of time (S. Chapman, pers. comm., August 2021) making the comparison even more challenging. The right forefin of NHMUK PV OR 14553 is complete and composed of more than 25 elements on the longest digit (Fig. 8A); however, the authenticity of this trait has been questioned (Chapman & Doyle, 2002; Maisch, 2010; Lomax, 2019). If genuine,

its length would represent an apomorphy since the number of elements in the longest digit in many early neoichthyosaurians does not exceed 20 (Motani, 1999a; Swaby & Lomax, 2020). Moreover, this condition looks more similar to *Stenopterygius uniter* (von Wurstemberger 1876), which has an elongated forefin (Maxwell, 2012). The left side of the skull is poorly preserved (Fig. 8), which restricts our comparisons with the holotype of *T. zetlandicus* (CAMSM J35176). Nevertheless, some remaining elements allow to differentiate the two specimens. Firstly, the most noticeable difference concerns the nasal. In *T. zetlandicus* this structure anteriorly ends as far as the maxilla and is not anterodorsally extended (Figs 2, 3A, B), whereas in '*I.*' *acutirostris*, the nasal, even if it is incomplete, seems to anteriorly end further than the maxilla (Fig. 8). This condition in '*I.*' *acutirostris* is more similar to the rest of Early Jurassic parvipelvians (Maisch, 2008; Maxwell *et al.*, 2012; Lomax & Massare, 2016; Maxwell & Cortés, 2020) with the exception of *Suevoleviathan* (Maisch, 2001). The morphology of the jugal also seems to differ in that the posterior extremity would not be notched (Fig. 8B). In NHMUK PV OR 14553, the postfrontal does not bear a prominent ridge on the anterior margin of the supratemporal fenestra (Fig. 8B), which is a distinctive feature of *T. zetlandicus*. Concerning cranial dimensions, the length of the postorbital region is larger compared to the diameter of the orbit than in *T. zetlandicus* (~0.8 for '*I.*' *acutirostris* vs. ~0.5 for *T. zetlandicus*; see Supporting Information, Table S1) even if the skull appears to be smaller in '*I.*' *acutirostris.* The taxonomic decisions in this paper require the assessment of the possible influence of ontogeny in driving the differences we observe between the holotype of '*I.*' *acutirostris*, which is small, and the holotype of *T. zetlandicus*. To do so, we assess the ontogenetic stage of the holotype of '*I.*' *acutirostris* by analysing the relative diameter of the sclerotic ring and the sclerotic aperture. This analysis has been used in the past to segregate juveniles (and supposed deep divers) from adults in neoichthyosaurians.

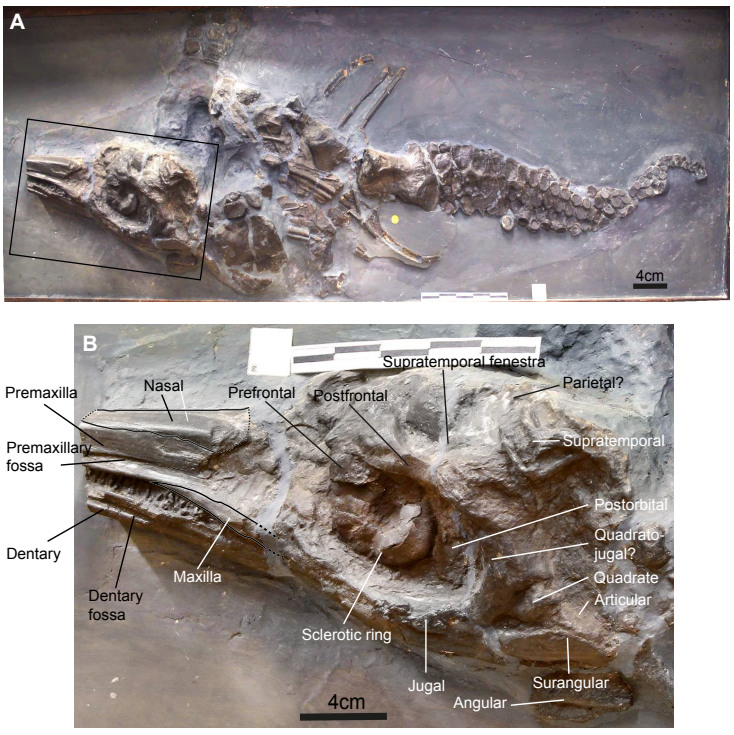

Figure 8. Photograph of the holotype of '*Ichthyosaurus*' *acutirostris* (NHMUK PV OR 14553). A, the whole specimen. B, interpretation of the skull.

Indeed, the orbit is nearly (Fernández *et al.*, 2005; Fischer *et al.*, 2013). Indeed, the orbit is nearly completely filled by the sclerotic ring in juveniles and deep divers, whereas in Indeed, the orbit is nearly completely filled by the sclerotic ring in juveniles and deep divers, whereas in non- deep diving adult forms, the sclerotic rings tend to occupy a smaller area within the orbit. Our measurements (taking into account that the postorbital has been displaced in NHMUK PV OR 14553) place of the holotype of '*I*'. *acutirostris* well within the adult ontogenetic stage (Fig. 11). According to these results, the differences in size and morphology between the holotype of '*I.*' *acutirostris* and the holotype of *T. zetlandicus* cannot be regarded as driven by osteological immaturity.

Our morphological comparison, albeit limited, of *T. zetlandicus* as a junior synonym of '*I.*' *acutirostris* is untenable. The other material referred to '*I.*' *acutirostris* needs a thorough reinvestigation once the material is accessible again (Maisch, 2010; Swaby & Lomax, 2020). Like Maisch (2010), we suggest removing '*I.*' *acutirostris* from *Temnodontosaurus* and placing it as *species inquirenda*, as *Ichthyosaurus acutirostris* according the initial assignment given by Owen (1840).

RESULTS

Phylogenetic analyses

Phylogenetic analyses under implied weighting maximum parsimony yielded 18 most-parsimonious trees (MPTs) with k = 12, each having a length of 68.312. The Consistency Index was 0.191 and the Retention Index was 0.644. Analyses conducted with k=6and k=9 generated one MPT each with a length of 102.201 and 81.639, respectively (these topologies are presented in Supporting Information, Figs S2, S3). In all of our MPTs, *T. zetlandicus* is recovered as a member of *Temnodontosaurus*, being systematically grouped within a number of species currently referred to as *Temnodontosaurus.* Indeed, with k = 6 and 9, this species is considered to be the sister taxon of *T. trigonodon*, while *T. nuertingensis* is the sister taxon of *T. zetlandicus* with k = 12 and also closely related to *T. trigonodon*. Nevertheless, these relationships are not well supported by the symmetric resampling value [under 50%, as is the case for nearly all nodes of the phylogeny. Similar low values have been obtained on a previous version of the data set by Moon (2017)]. In MPTs generated with K = 12, the synapomorphies that unite these three species are the extension of the jugal that reaches the anterior end of the lachrymal (30.1) and the extensive participation of the splenial in the mandibular symphysis (122.0); the absence of a complexly lobate shape of its external naris (26.0) unites *T. zetlandicus* and *T. nuertingensis*. In all topologies, members of *Temnodontosaurus* appeared well clustered yet not monophyletic. This is essentially due to the fluctuating position of *T. azerguensis*, which is found to be more basal than the other species of *Temnodontosaurus* ink=6andmorederivedink=12,where it forms a clade with a diminutive version of Leptonectidae (*Leptonectes moorei* + *Leptonectes tenuirostris* (McGowan & Milner, 1999) + *Excalibosaurus costini* (McGowan, 1986)). As a whole, Leptonectidae is recovered more as a grade rather than a clade in k = 12 (Fig. 9), but not when homoplastic characters are more strongly penalized (k = 6 and k = 9; Supporting Information, Figs S2, S3). The polyphyletic status of *Temnodontosaurus* is also attributable to the inclusion of *Suevoleviathan* in k = 9

and in k = 12. In order to statistically test the monophyly of *Temnodontosaurus*, we computed a Templeton's parametric test with a tree in which the monophyly of the genus was forced (under k = 12). The result of the test indicated that this solution is statistically indistinguishable (*P*-value > 0.05) from our most parsimonious tree generated without monophyly constraints. A monophyletic *Temnodontosaurus* is thus a suboptimal yet fully probable topology with the data presently at hand (see Supporting Information, Fig. S4). The position of *Temnodontosaurus*—or *Temnodontosaurus*-like forms [the temnodontosaurids or temnodontosauoids of some authors (McGowan, 1994; Maisch & Matzke, 2000; McGowan & Motani, 2003)]—fluctuates within neoichthyosaurians, depending on the penalty applied to homoplastic characters. Indeed, with k = 6, a clade comprising many species of *Temnodontosaurus* is found to be one of the most primitive clades of the Early Jurassic, as previously inferred (Sander, 2000; Maisch & Matzke, 2000; Maxwell *et al.*, 2012; Fischer *et al.*, 2016; Moon, 2017; Zverkov & Jacobs, 2020). In k = 9 and 12, Ichthyosauridae appeared to be the basalmost family of neoichthyosaurians, as in Maxwell & Cortés (2020).

Bayesian inference (Fig. 10) provides a comparable topology to those generated in an implied weighting maximum parsimony framework with high values of k (9 and 12). *Temnodontosaurus zetlandicus* is also recovered within a clade grouping many other species currently referred to as *Temnodontosaurus*, as well as *Suevoleviathan.* Within this clade, *T. zetlandicus* forms a moderately well-supported (posterior probability of 65%) clade grouping *T. trigonodon* and *T. platyodon* and appears more derived than *T. nuertingensis.* Members of the genus appear well clustered and are not considered more primitive than Ichthyosauridae (*Ichthyosaurus*, *Protoichthyosaurus*) which is the most basal clade of Jurassic parvipelvians as shown in our maximum parsimony analyse, comparable to the results of Moon (2017) and Maxwell & Cortes (2020). Furthermore, *Temnodontosaurus* is still recovered as polyphyletic for the same reasons as in maximum parsimony analyses: *Suevoleviathan* is included within *Temnodontosaurus* and *T. azerguensis* clusters with leptonectids.

DISCUSSION

The validity and relationships of *Temnodontosaurus zetlandicus*

Our osteological comparative study of *T. zetlandicus* and the comparison with the holotype of '*I.*' *acutirostris* indicates the validity of *T. zetlandicus* and provide new evidence for its placement in *Temnodontosaurus.* Indeed, this species shares with other temnodontosaurids a large skull, a low maxilla that anteriorly ends as far as the nasal (Figs 2, 3A, B; Martin *et al.*, 2012; Swaby & Lomax, 2020) and a parasphenoid that crosses the entire length of the basisphenoid (Fig. 3C, D) which forces a paired carotid foramina (Fraas, 1913; von Huene, 1931; Godefroit, 1993a; Maisch & Matzke, 2000; Maisch, 2002; Martin *et al.*, 2012). These assumptions are also confirmed by our phylogenetic analyses as *T. zetlandicus* is recovered as closely related to *T. nuertingensis* and *T. trigonodon*, both in maximum parsimony (Fig. 9) and in Bayesian inference (Fig. 10). Morphologically, these three species possess a similar rostrum with a jugal that anteriorly contacts the subnarial process of the premaxilla and partially covers the maxilla (Maisch &

Hungerbühler, 1997; Pardo-Pérez *et al.*, 2018). Nonetheless, some differences are noticeable. The maxilla of *T. nuertingensis* is dorsoventrally higher than in *T. zetlandicus* as it nearly reaches the external naris and on the palate region, the vomer is larger and almost excludes contact between the pterygoid and the palatine (Maisch & Hungerbühler, 1997). Furthermore, *T. nuertingensis* is older, currently only found in the Lower Pliensbachian strata of Germany (Maisch & Hungerbühler, 1997); yet the incompleteness of the holotype (SMNS 13488) severely limits our comparisons. For these reasons, further investigations are therefore required to better understand the relationship between *T. zetlandicus* and *T. nuertingensis.* The cranial morphology of *T. trigonodon* is better known since many specimens have been found in western Europe (McGowan, 1996a). Our osteological comparison highlighted numerous common features between *T. zetlandicus* and *T. trigonodon* (Fig. 12), other than the anterior shape of the jugal, largely covering the maxilla. Indeed, in addition of a comparable configuration of the braincase and the palate, these two species share a similar architecture for the postorbital region, with an species largely covering the maxilla. Indeed, in addition of a comparable configuration of the braincase and the palate, these two share a similar architecture for the postorbital region, with an anteroposteriorly and dorsally well-extended quadratojugal, a triangular squamosal and a notched posterior extremity of the jugal. The architecture of the skull roof is also distinctive as it is marked by the presence of a prominent mediolaterally oriented ridge on the postfrontal, forming the anterior margin of the supratemporal fenestra and a prominent parasagittal crest on the parietal that anteriorly ends in a slender process slightly covering the slender

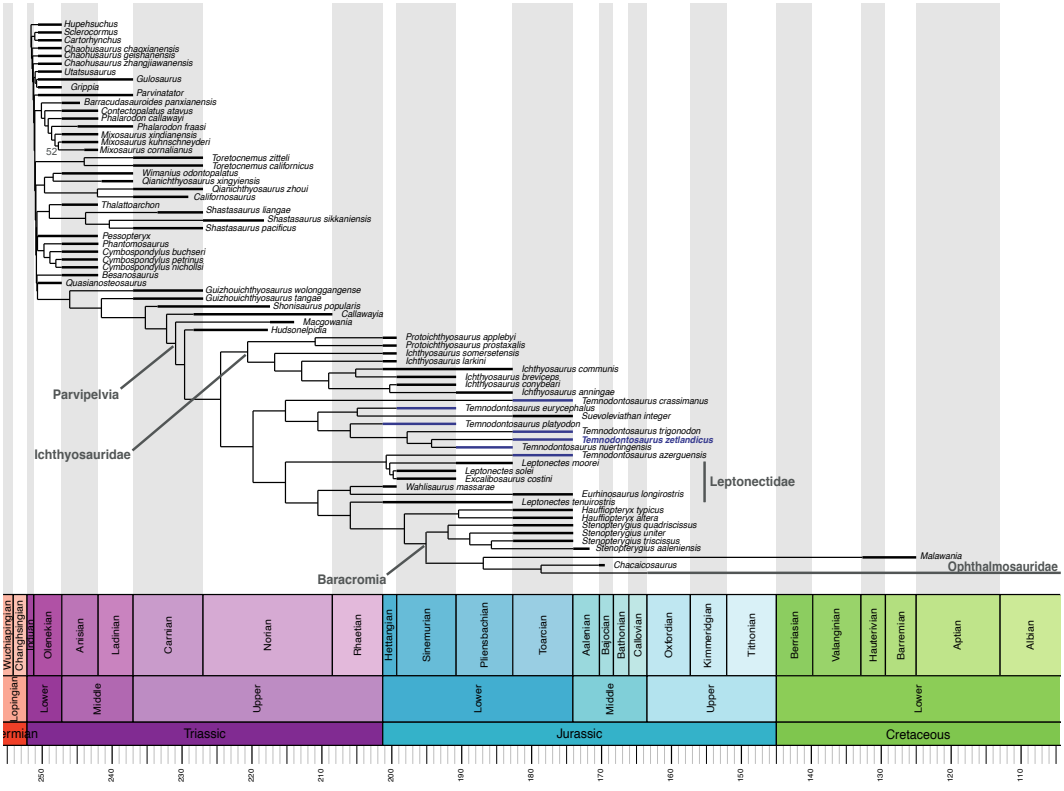

Figure 9. Time-scaled phylogeny of ichthyopterygians arising from implied weighting (k = 12) maximum parsimony analysis, in 'equal' reconstruction branches lengths. Branch values of resampling ≥ 50 are indicated on the branches leading their corresponding nodes.

frontal that only reaches the anterior margin of the parietal foramen. These common features on the skull roof only occur in *T. trigonodon*, *T. zetlandicus* and *T.* cf. *zetlandicus* (MNHNL TU885) (Figs 7, 12). Despite these similarities, *T. zetlandicus* differs from *T. trigonodon* in a number of aspects (Fig. 12). The size of the skull is effectively smaller (~1 m in *T. zetlandicus* vs. > 1.5 m in *T. trigonodon*; see Supporting Information, Table S1), as is the relative size of the postorbital region (length of the postorbital region/length of the orbit ratio: ~0.5 for *T. zetlandicus* vs. ~0.8–0.9 for *T. trigonodon*; see Supplementary Information, Table S1). These differences could be due to variation in ontogenetic stages even if we are confident that CAMSM J35176 represents an adult (see above).

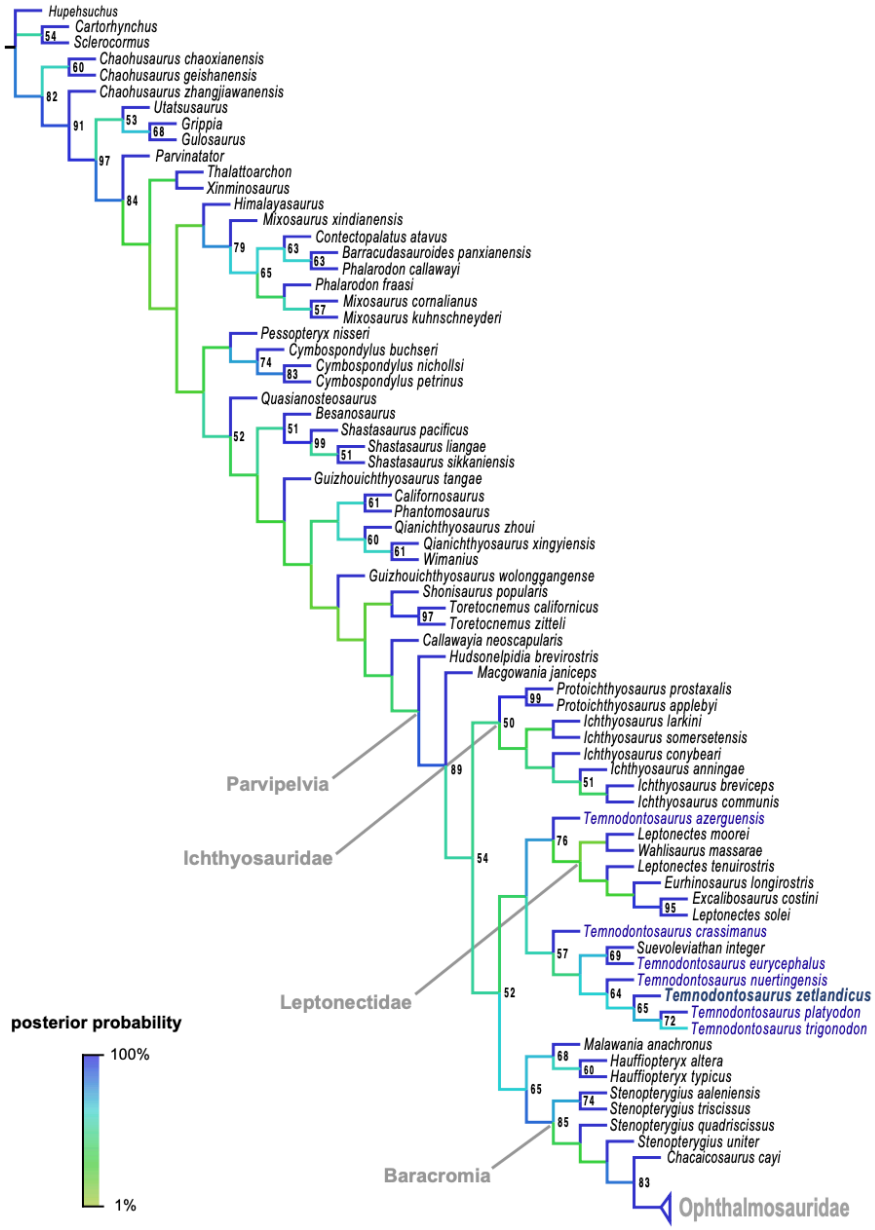

Figure 10. Phylogeny of ichthyopterygians arising from Bayesian inference. Colour coding indicates percentages of posterior probabilities for each branch. Percentages of posterior probabilities ≥ 50 are indicated in their corresponding nodes.

In addition to these variations in skull proportions, the lacrimal is notched and less extended dorsally in T. zetlandicus and the nasal, which does not possess a postnarial descending process, overlaps the postfrontal by two processes, the most lateral being digitated. Therefore, we consider these differences as sufficient to classify T. zetlandicus and T. trigonodon as two distinct but closely related species from the Early Toarcian of western Europe.

Taxonomic content and phylogenetic relationships of *Temnodontosaurus*

Despite recent progress (Swaby & Lomax, 2020) and our propositions (see above), *Temnodontosaurus* remains a loosely defined entity for which it is still complex to find compelling apomorphies (Swaby & Lomax, 2020; but see the emended diagnosis of the genus in Martin *et al.*, 2012). Whilst awaiting autapomorphy- and synapomorphy-based diagnoses, *Temnodontosaurus* as currently defined is possibly a wastebasket taxon containing large neoichthyosaurians from the Lower Jurassic (Swaby & Lomax, 2020). However, some species such as *T. crassimanus*, *T. platyodon*, *T. trigonodon* and *T. zetlandicus* appear sufficiently phylogenetically stable and well preserved, in contrary to *T. azerguensis*, *T. eurycephalus* McGowan, 1974 and *T. nuertingensis*, to form the core of *Temnodontosaurus*. Therefore, we suggest that diagnostic revisions of the genus be based on osteological examination of these species. complex to find compelling apomorphies (Swaby & Lomax, 2020; but see the emended diagnosis of the genus in Martin *et al.*, 2012). Whilst awaiting autapomorphy- and synapomorphy-based diagnoses, *Temnodontosaurus* as currently defined is possibly a wastebasket taxon containing large neoichthyosaurians from the Lower Jurassic (Swaby & Lomax, 2020). However, some species such as *T. crassimanus*, *T. platyodon*, *T. trigonodon* and *T. zetlandicus* appear sufficiently phylogenetically stable and well preserved, in contrary to *T. azerguensis*, *T. eurycephalus* McGowan, 1974 and *T. nuertingensis*, to form the core of *Temnodontosaurus*. Therefore, we suggest that diagnostic revisions of the genus be based on osteological examination of these species. Members of *Temnodontosaurus* are still relatively well clustered among Jurassic parvipelvians in all of our phylogenetic analyses. This demonstrates that despite a diagnosis based on mainly phenetics, species currently included in the genus seem to be phylogenetically close even if they do not form a monophyletic entity. Nevertheless, the lack of statistical support demonstrates that interrelationships of *Temnodontosaurus* and phylogenetic re-evluations that are ongoing (Martin *et al.*, 2012; Maxwell *et al.*, 2012; Fischer *et al.*, 2013; Marek *et al.*,

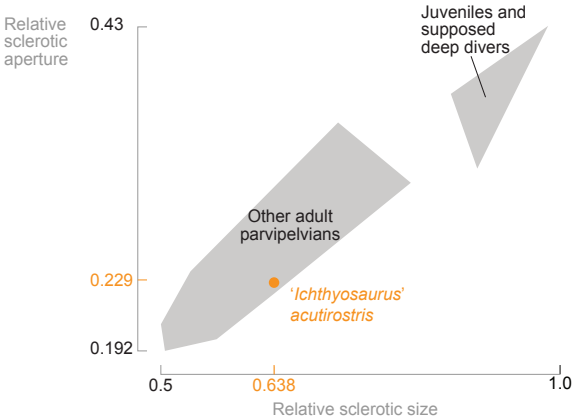

Figure 11. Sclerotic aperture and external sclerotic diameters of various parvipelvians relative to orbit diameter. The grey colour represents the repartition of the species included in the study of Fernández *et al.* (2005) and the orange colour is relative to the values and the position of '*Ichthyosaurus*' *acutirostris*. Modified from Fischer *et al.* (2013). Values for '*I*'. *acutirostris*: sclerotic aperture diameter: 17.2 mm; external sclerotic diameter: 48.8 mm; orbit diameter: 76.5 mm.

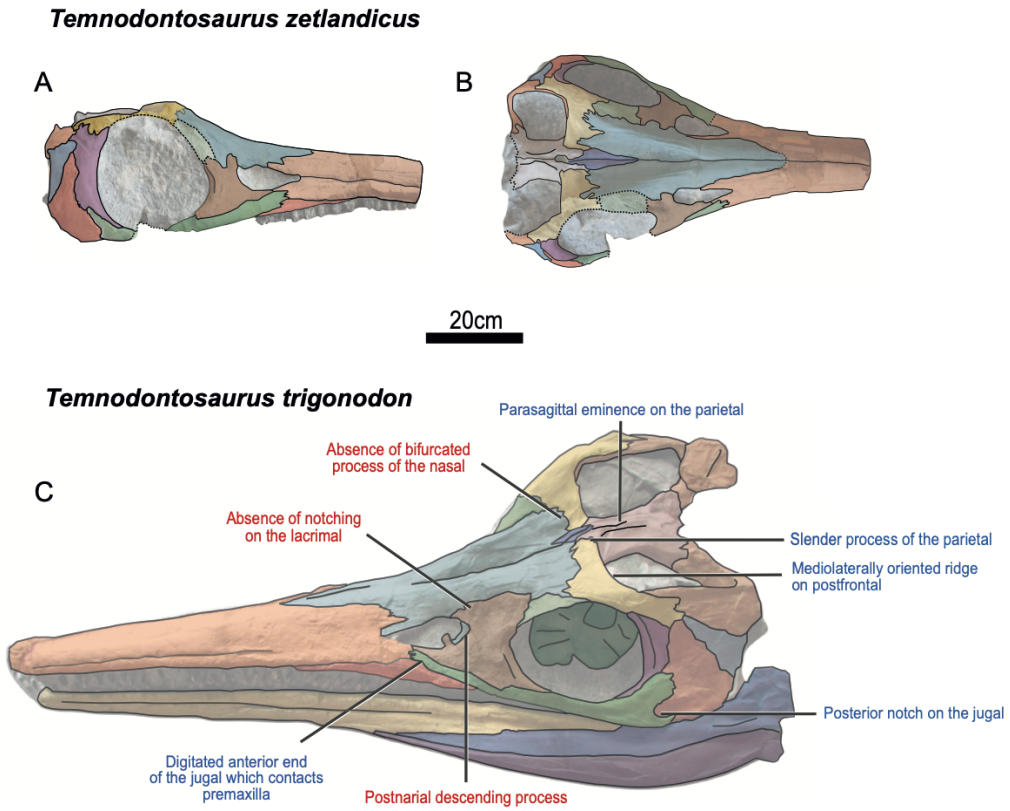

Figure 12. *Temnodontosaurus zetlandicus* comb. nov. and *Temnodontosaurus trigonodon*. A, B, interpretation of the lateral and the dorsal view of the holotype of *Temnodontosaurus zetlandicus* comb. nov. (CAMSM J35176), respectively. C, interpretation of *Temnodontosaurus trigonodon* (SMNS 15950), modified from Swaby & Lomax (2020). The blue-coloured labels indicate shared features whereas the red-coloured labels indicate morphological differences with *Temnodontosaurus zetlandicus* comb. nov.

2015; Lomax, 2016; Maxwell, 2018; Lomax *et al.*, 2019; Swaby & Lomax, 2020) to find new and more suitable characters in order to clarify the tempo and the shape of the neoichthyosaurian radiation.

CONCLUSION

This paper provides an osteological redescription the holotype of '*Ichthyosaurus*' *zetlandicus*, which was previously synonymized under '*Ichthyosaurus*' *acutirostris.* Instead, '*I.*' *zetlandicus* shares morphological traits with *Temnodontosaurus nuertingensis* and *T. trigonodon* and is phylogenetically close to these two species. We thus reassign '*Ichthyosaurus*' *zetlandicus* to *T. zetlandicus* and we also refer a new specimen from the Toarcian of Luxembourg to *Temnodontosaurus* cf. *zetlandicus*. Our phylogenetic analyses using multiple optimality criteria suggest that even if *Temnodontosaurus* as currently defined is not monophyletic, many of its members are relatively well clustered among Early Jurassic parvipelvians and could serve as a core to redefine the genus. Therefore, this study marks another step in revising the problematic taxonomy of *Temnodontosaurus* and provides new information about its interrelationships, despite the need for additional data to recover a stable phylogeny.

ACKNOWLEDGMENTS

We would like to thank Matt Riley (CAMSM), Erin Maxwell (SMNS) and Brigitte Eichner-Grünbeck (PB) for the opportunity to access to materials. AL would like to thank Emily Swaby for the authorisation to modify the figure which includes the specimen SMNS 15950. RFB would like to thank Eckhard Mönnig (Naturkunde-Museum Coburg) for his assistance facilitating the visit to PB. The work of AL and RFB was supported by the Fond de la Recherche Scientifique doctoral (F.R.S– FNRS) FRIA grant (AL grant number FC38761 and RFB grant number FC 23645) and the Yorkshire Geological Society Fearnsides Award (RFB). We would also like to thank Dean Lomax and Erin Maxwell again for their thorough reviews which have greatly contributed to the improvement of this paper.

REFERENCES

Bapst DW. 2012. Paleotree: an R package for paleontological and phylogenetic analyses of evolution. *Methods in Ecology and Evolution* **3:** 803–807.

Bardet N. 1992. Stratigraphic evidence for the extinction of the ichthyosaurs. *Terra Nova* **4:** 649–656.

Bell MA, **Lloyd GT. 2015.** strap: an R package for plotting phylogenies against stratigraphy and assessing their stratigraphic congruence. *Palaeontology* **58:** 379–389.

Benton MJ, **Spencer PS. 1995.** Fossil reptiles of Great Britain. Volume 10. London: Chapman & Hall, pp XII, 386. *Archives of Natural History* **23:** 150–151.

Benton MJ, **Taylor MA. 1984.** Marine reptiles from the Upper Lias (Lower Toarcian, Lower Jurassic) of the Yorkshire coast. *Proceedings of the Yorkshire Geological Society* **44:** 399–429.

Bindellini G, **Wolniewicz AS**, **Miedema F**, **Scheyer TM**, **Dal Sasso C. 2021.** Cranial anatomy of *Besanosaurus leptorhynchus* Dal Sasso & Pinna, 1996 (Reptilia: Ichthyosauria) from the Middle Triassic Besano Formation of Monte San Giorgio, Italy/Switzerland: taxonomic and palaeobiological implications. *PeerJ* **9:** e11179.

Blainville HMD. 1835. Description de quelques espèces de reptiles de la Californie: précédée de l'analyse d'un système général d'herpétologie et d'amphibiologie. *Nouvelles Annales du Muséum d'Histoire Naturelle, Paris* **4:** 233–296.

Böttcher R. 1989. Über die Nahrung eines *Leptopterygius* (Ichthyosauria, Reptilia) aus dem süddeutschen Posidonienschiefer (Unterer Jura) mit Bemerkungen über den Magen der Ichthyosaurier. *Stuttgarter Beiträge zur Naturkunde, Serie B (Geologie und Paläontologie)* **155:** 1–19.

Caine H, **Benton MJ. 2011.** Ichthyosauria from the Upper Lias of Strawberry Bank, England. *Palaeontology* **54:** 1069–1093.

Chapman SD, **Doyle AM. 2002.** *An initial investigation into the acquisition and conservation history of the fossil marine reptile* Stenopterygius acutirostris *(Owen) from the Upper Liassic near Whitby, Yorkshire, England*.

Dick DG, **Maxwell EE. 2015.** The evolution and extinction of the ichthyosaurs from the perspective of quantitative ecospace modelling. *Biology Letters* **11:** 20150339.

Fernández M. 1994. A new long-snouted ichthyosaur from the Early Bajocian of Neuquén basin (Argentina). *Ameghiniana* **31:** 291–297.

Fernández M, **Archuby F**, **Talevi M**, **Ebner R. 2005.** Ichthyosaurian eyes: paleobiological information content in the sclerotic ring of *Caypullisaurus*

(Ichthyosauria, Ophthalmosauria). *Journal of Vertebrate Paleontology* **25:** 330–337.

Fischer V. 2016. Taxonomy of *Platypterygius campylodon* and the diversity of the last ichthyosaurs. *PeerJ* **4:** 1–21.

Fischer V, **Appleby RM**, **Naish D**, **Liston J**, **Riding JB**, **Brindley S**, **Godefroit P. 2013.** A basal thunnosaurian from Iraq reveals disparate phylogenetic origins for Cretaceous ichthyosaurs. *Biology Letters* **9:** 1–6.

Fischer V, **Arkhangelsky MS**, **Uspensky GN**, **Stenshin IM**, **Godefroit P. 2013.** A new Lower Cretaceous ichthyosaur from Russia reveals skull shape conservatism within Ophthalmosaurinae. *Geological Magazine* **151:** 60–70.

Fischer V, **Bardet N**, **Benson RBJ**, **Arkhangelsky MS**, **Friedman M. 2016.** Extinction of fish-shaped marine reptiles associated with reduced evolutionary rates and global environmental volatility. *Nature Communications* **7:** 10825.

Fischer V, **Benson RBJ**, **Zverkov NG**, **Soul LC**, **Arkhangelsky MS**, **Lambert O**, **Stenshin IM**, **Uspensky GN**, **Druckenmiller PS. 2017.** Plasticity and convergence in the evolution of short-necked plesiosaurs. *Current Biology* **27:** 1667–1676.

Fischer V, **Cappetta H**, **Vincent P**, **Garcia G**, **Goolaerts S**, **Martin JE**, **Roggero D**, **Valentin X. 2014.** Ichthyosaurs from the French Rhaetian indicate a severe turnover across the Triassic–Jurassic boundary. *Naturwissenschaften* **101:** 1027–1040.

Fischer V, **Maclaren JA**, **Bennion RF**, **Druckenmiller PS**, **Benson RBJ. 2020.** The macroevolutionary landscape of short-necked plesiosaurians. *Scientific Reports* **10:** 16434.

Fischer V, **Maisch MW**, **Naish D**, **Kosma R**, **Liston J**, **Joger U**, **Krüger FJ**, **Pardo Pérez J**, **Tainsh J**, **Appleby RM. 2012.** New ophthalmosaurid ichthyosaurs from the European Lower Cretaceous demonstrate extensive ichthyosaur survival across the Jurassic-Cretaceous boundary. *PLoS One* **7:** e29234.

Fischer V, **Masure E**, **Arkhangelsky MSMS**, **Godefroit P. 2011.** A new Barremian (Early Cretaceous) ichthyosaur from western Russia. *Journal of Vertebrate Paleontology* **31:** 1010–1025.

Fischer V, **Weis R**, **Thuy B. 2021.** Refining the marine reptile turnover at the Early-Middle Jurassic transition. *PeerJ* **9:** e10647.

Fraas EE. 1913. Ein unverdrückter *Ichthyosaurus*-Schädel. *Jahreshefte des Vereins für Vaterländische Naturkunde in Württemberg* **69:** 1–12.

Godefroit P. 1993a. Les grands ichthyosaures sinémuriens d'Arlon. *Bulletin de l'Institut Royal des Sciences Naturelles de Belgique Sciences de la Terre* **63:** 25–71.

Godefroit P. 1993b. The skull of *Stenopterygius longifrons* (Owen, 1881). *Revue de Paléobiologie de Genève volume spécial* **7:** 67–84.

Godefroit P. 1994. Les reptiles marins du Toarcien (Jurassique inférieur) belgo-luxembourgeois. *Mémoires pour Servir à l'Explication des Cartes Géologiques et Minières de la Belgique* **39:** 98.

Goloboff PA, **Catalano SA. 2016.** TNT version 1.5, including a full implementation of phylogenetic morphometrics. *Cladistics* **32:** 221–238.

Goloboff PA, **Farris JS**, **Källersjö M**, **Oxelman B**, **Ramìrez MJ**, **Szumik CA. 2003.** Improvements to resampling measures of group support. *Cladistics* **19:** 324–332.

Goloboff PA, **Farris JS**, **Nixon KC. 2008.** TNT, a free program for phylogenetic analysis. *Cladistics* **24:** 774–786.

Goloboff PA, **Torres A**, **Arias JS. 2018.** Weighted parsimony outperforms other methods of phylogenetic inference under models appropriate for morphology. *Cladistics* **34:** 407–437.

Hermoso M, **Delsate D**, **Baudin F**, **Le Callonnec L**, **Minoletti F**, **Renard M**, **Faber A. 2014.** Record of Early Toarcian carbon cycle perturbations in a nearshore environment: the Bascharage section (easternmost Paris Basin). *Solid Earth* **5:** 793–804.

Hodges P, **Simms M**, **Page K. 2004.** 1. British Lower Jurassic stratigraphy: an introduction. *Geological Conservation Review Series* **30:** 28–37.

von Huene F. 1922. Die Ichthyosaurier des Lias und ihre Zusammenhänge. In: *Monographien zur Geologie und Paläontologie, 1*. Berlin: Borntraeger.

von Huene F. 1931. Neue Ichthyosaurier aus Württemberg. *Neues Jahrbuch für Mineralogie, Geologie und Paläontologie. Beilage. Abteilung B* **65:** 305–320.

Johnson MM, **Young MT**, **Brusatte SL**, **Thuy B**, **Weis R. 2019.** A catalogue of teleosauroids (Crocodylomorpha: Thalattosuchia) from the Toarcian and Bajocian (Jurassic) of southern Luxembourg. *Historical Biology* **31:** 1179–1194.

Kelley NP, **Pyenson ND. 2015.** Evolutionary innovation and ecology in marine tetrapods from the Triassic to the Anthropocene. *Science* **348:** aaa3716.

Lomax DR. 2016. A new leptonectid ichthyosaur from the Lower Jurassic (Hettangian) of Nottinghamshire, England, UK, and the taxonomic usefulness of the ichthyosaurian coracoid. *Journal of Systematic Palaeontology* **15:** 387–401.

Lomax DR. 2019. Ichthyopterygia. In: Lord AR, Munt M, eds. *Fossils from the Lias of the Yorkshire Coast.* London: The Palaeontological Association, 317–331.

Lomax DR, **Massare JA. 2016.** Two new species of *Ichthyosaurus* from the lowermost Jurassic (Hettangian) of Somerset, England. *Papers in Palaeontology* **3:** 1–20.

Lomax DR, **Massare JA. 2018.** A second specimen of *Protoichthyosaurus applebyi* (Reptila: Ichthyosauria) and additional information on the genus and species. *Paludicola* **11:** 164–178.

Lomax DR, **Massare JA**, **Evans M. 2020.** New information on the skull roof of *Protoichthyosaurus* (Reptilia: Ichthyosauria) and intraspecific variation in some dermal skull elements. *Geological Magazine* **157:** 640–650.

Lomax DR, **Porro LB**, **Larkin NR. 2019.** Descriptive anatomy of the largest known specimen of *Protoichthyosaurus prostaxalis* (Reptilia: Ichthyosauria) including computed tomography and digital reconstruction of a three-dimensional skull. *PeerJ* **7:** e6112.

Lydekker R. 1889. Palaeozoology: Vertebrata. In: *A manual of palaeontology for the use of students with a general introduction on the principles of palaeontology*, *3rd edn*. Edinburgh: W. Blackwood, 889–1464.

Maisch MW. 1997. A case against a diapsid origin of the Ichthyosauria. *Neues Jahrbuch für Geologie und Paläontologie, Abhandlungen* **205:** 111–127.

Maisch MW. 1998a. A new ichthyosaur genus from the Posidonia Shale (Lower Toarcian, Jurassic) of Holzmaden, SW-Germany with comments on the phylogeny of post- Triassic ichthyosaurs. *Neues Jahrbuch für Geologie und Paläontologie, Abhandlungen* **209:** 47–78.

Maisch MW. 1998b. Short review of the ichthyosaurs of the Posidonienschiefer with remarks on the taxonomy of the Stenopterygiidae and Temnodontosauridae. *Neues Jahrbuch für Geologie und Paläontologie, Abhandlungen* **209:** 401–431.

Maisch MW. 2001. Neue Exemplare der seltenen Ichthyosaurier Gattung *Suevoleviathan* Maisch 1998 aus dem Unteren Jura von Südwestdeutschland. *Geologica et Palaeontologica* **35:** 145–160.

Motani R. 1999b. Phylogeny of the Ichthyopterygia. *Journal of Vertebrate Paleontology* **19:** 473–496.

Motani R. 2005. Evolution of fish-shaped reptiles (Reptilia: Ichtyopterygia) in their physical environments and constraints. *Annual Review of Earth and Planetary Sciences* **33:** 395–420.

Motani R, **Jiang D**, **Tintori A**, **Ji C**, **Huang J. 2017.** Pre- versus post-mass extinction divergence of Mesozoic marine reptiles dictated by time-scale dependence of evolutionary rates. *Proceedings of the Royal Society series B* **284:** 20170241.

Owen R. 1865–1881. *A monograph of the fossil Reptilia of the Liassic Formations, part third:* Plesiosaurus, Dimorphodon*, and* Ichthyosaurus. London: Monographs of the Palæontographical Society, 12–130.

Paradis E, **Claude J**, **Strimmer K. 2004.** APE: analyses of phylogenetics and evolution in R language. *Bioinformatics* **20:** 289–290.

Pardo-Pérez JM, **Kear BP**, **Mallison H**, **Gómez M**, **Moroni M**, **Maxwell EE. 2018.** Pathological survey on *Temnodontosaurus* from the Early Jurassic of southern Germany. *PLoS One* **13:** e0204951.

Pol D, **Escapa IH. 2009.** Unstable taxa in cladistic analysis: identification and the assessment of relevant characters. *Cladistics* **25:** 515–527.

Powell J. 2010. Jurassic sedimentation in the Cleveland Basin: a review. *Proceedings of the Yorkshire Geological Society* **58:** 21–72.

Ronquist F, **Klopfstein S**, **Vilhelmsen L**, **Schulmeister S**, **Murray DL**, **Rasnitsyn AP. 2012.** A total-evidence approach to dating with fossils, applied to the early radiation of the hymenoptera. *Systematic Biology* **61:** 973–999.

Sander PM. 2000. Ichthyosauria: their diversity, distribution, and phylogeny. *Paläontologische Zeitschrift* **7:** 1–35.

Seeley HG. 1880. On the skull of an *Ichthyosaurus* from the Lias of Whitby,apparently indicating a new species (*I. zetlandicus*, Seeley), preserved in the Woodwardian Museum of the University of Cambridge. *Quarterly Journal of the Geological Society* **36:** 635–647.

Smith MR. 2019. Bayesian and parsimony approaches reconstruct informative trees from simulated morphological datasets. *Biology Letters* **15:**20180632.

Streitz JC. 1983. *Auf Fossiliensuche in Luxemburg. Entstehung und Beschreibung einer bemerkenswerten Privatsammlung*. Luxembourg: Imprimerie Saint-Paul.

Swaby EJ, **Lomax DR. 2020.** A revision of *Temnodontosaurus crassimanus* (Reptilia: Ichthyosauria) from the Lower Jurassic (Toarcian) of Whitby, Yorkshire, UK. *Historical Biology* **33:** 2715–2731.

Templeton AR. 1983. Phylogenetic inference from restriction endonuclease cleavage site maps with particular reference to the evolution of humans and the apes. *Evolution* **37:** 221–244.

Theodori C. 1843. Über einen kolossalen *Ichthyosaurus trigonodon*. *Gelehrte Anzeigen der Königlich Bayerischen Akademie der Wissenschaften, München* **16:** 906–911.

Thorne PM, **Ruta M**, **Benton MJ. 2011.** Resetting the evolution of marine reptiles at the Triassic-Jurassic boundary. *Proceedings of the National Academy of Sciences of the USA* **108:** 8339–8344.

Vincent P, **Taquet P**, **Fischer V**, **Bardet N**, **Falconnet J**, **Godefroit P. 2014.** Mary Anning's legacy to French vertebrate palaeontology. *Geological Magazine* **151:** 7–20.

Vincent P, **Weiss R**, **Kronz G**, **Delsate D. 2017.** *Microcleidus melusinae*, a new plesiosaurian (Reptilia, Plesiosauria) from the Toarcian of Luxembourg. *Geological Magazine* **156:** 99–116.

Zverkov N, **Jacobs M. 2020.** Revision of *Nannopterygius* (Ichthyosauria: Ophthalmosauridae): reappraisal of the 'inaccessible' holotype resolves a taxonomic tangle and reaveals an obscure ophthalmosaurid lineage with a wide distribution. *Zoological Journal of the Linnean Society* **191:** 228–2

SUPPORTING INFORMATION

Additional Supporting Information may be found in the online version of this article at the publisher's web-site:

File S1. Character-taxon matrix used for phylogenetic analyses.
File S2. Character-taxon matrix and parameters for Bayesian analysis. Character list copied from the study of Maxell & Cortés (2020) and character coding revision.
Figure S1. Schematic stratigraphic log of the Whitby coastal section in North Yorkshire (UK).
Figure S2. Time-scaled phylogenetic tree, arising from implied weighting (k = 6) maximum parsimony analysis, in 'equal' reconstruction branch lengths.
Figure S3. Time-scaled phylogenetic tree in which the monophyly of *Temnodontosaurus* is forced, arising from implied weighting (k = 9) maximum parsimony analysis, in 'equal' reconstruction branch lengths.
Figure S4. Time-scaled phylogenetic tree arising from implied weighting (k = 12) maximum parsimony analysis, in 'equal' reconstruction branch lengths.
Figure S5. Majority rule consensus cladogram generated with a Bayesian analysis.
Table S1. Selected measurements (mm) and notable cranial ratios between *T. zetlandicus*, '*I.*' *acutirostris* and *T. trigonodon.*